Radiographic Imaging and Finite Element Modeling Methods for Analysis of the Basilar Thumb Joint

By

Nolan Matthew Norton

Submitted to the graduate degree program in Bioengineering and the Graduate Faculty of the University of Kansas in partial fulfillment of the requirements for the degree of Master of Science.

_____

Chair: Dr. Kenneth Fischer

_____

Dr. Terence McIff

_____

Dr. Lisa Friis

Date Defended: 11/30/2018

The Thesis Committee for Nolan Matthew Norton

certifies that this is the approved version of the following thesis:

Radiographic Imaging and Finite Element Modeling Methods for Analysis of the Basilar Thumb Joint

_____

Chair: Dr. Kenneth Fischer

Date Approved: 12/14/2018

Abstract

Laxity of the stabilizing ligaments, specifically the anterior oblique ligament (AOL) and the dorsoradial ligament (DRL), is believed to play a major role in the development of osteoarthritis (OA) of the basilar thumb joint. Increased laxity of the stabilizing ligaments is believed to contribute to cartilage degeneration through dorsal translation of the metacarpal, increased shear stresses, and a shift in contact to areas of weaker cartilage. Stress radiographs during functional tasks, such as key pinch, can be used to help assess joint instability. Eleven cadaveric specimens were rigged to simulate key pinch, and a mobile C-arm was used to take a series of radiographic images with the joint capsule intact, opened, and after transection of the AOL. Images were taken from the anteroposterior (AP) view up to 60º toward the ulnar aspect of the arm to determine which angle allowed the best assessment of subluxation. The AP view showed the maximum amount of subluxation in a majority of the specimens. Subluxation significantly correlated with radiographic grades of OA but did not correlate with visual/arthroscopic grades of OA. Transection of the AOL did not have a significant effect on subluxation. Three-dimensional modeling techniques, such as finite element modeling, can be used to measure in vivo contact mechanics without disrupting the joint capsule and other supportive soft tissues. Models could have future clinical diagnostic and research applications, but they must first be validated against experimental data. Three specimens underwent MRI scanning in "relaxed" and "pinch" configurations to create finite element models for intact and open joint capsule simulations of key pinch. Model results were compared to experimental data collected by electronic sensors. Only measurements for contact force met validation criteria, and contact area was overestimated in every specimen. Contact measurements were not significantly affected by opening the joint capsule, but all four contact measures trended upward after opening the joint capsule. This supports the need for continued refinement of validation experimental methods and the benefits of computational modeling for future studies of contact mechanics.

Acknowledgements

We are only as strong as we are united, as weak as we are divided. – Albus Dumbledore

I would like to thank the Department of Orthopedic Surgery at the University of Kansas Medical Center whose funding made this research possible. I would also like to take a moment to express my sincere and upmost gratitude to my advisor at the University of Kansas, Dr. K. J. Fischer, for allowing me to work as a member of his lab. His mentorship, patience, kindness, consistent aide, and insights have made all of this research possible and have helped me to grow as both a researcher and as a person. I want to extend my gratitude towards Dr. T. McIff at the University of Kansas Medical Center. The privilege to work in his lab with him, his students, and the research resident Brandon Barnds allowed me to learn in an excellent research environment that helped me to find success with this project. I would also like to thank Dr. L. Friis for being a part of my committee and providing her knowledge and expertise with cadaveric testing to enhance the quality of this research. I am grateful for all of the support that I have received from all of my friends in the Bioengineering program and across the various disciplines at The University of Kansas. Their kindness and friendship along the way have made this journey possible. I must also thank my parents and the rest of my family for their encouragement and support. My mom's fighting spirit and determination throughout her battles with cancer over the past four of years have been an inspiration and reminder that no matter what circumstances we may be facing that we can always find a reason to smile and something for which to be thankful.

Table of Contents

Table of Figures/Tables

Chapter 1. Background

"In the absence of any other proof, the thumb alone would convince me of God's existence" – Isaac Newton

1.1 Anatomy of the Basilar Thumb Joint

The basilar thumb joint allows for opposition to the fingers, and thus it gives the ability to perform precision and power pinch [1]. The basilar thumb joint is also referred to as either the trapeziometacarpal (TMC) joint or the carpometacarpal (CMC) joint of the thumb. The primary bones that form the joint are the first metacarpal and trapezium (Figure 1.1). The scaphoid, trapezoid, and the second metacarpal are surrounding bones that help to form the adjacent trapeziotrapezoid, scaphotrapezial, and trapezial-second metacarpal joints which provide ligamentous attachments and stability for the base of the trapezium.

Figure 1.1 Oblique radiograph of the bones within and around the base of the thumb. Thumb Metacarpal = MC1, Trapezium = Tz, Scaphoid = S, Trapezoid = Td, and Second Metacarpal = MC2 (Used with permission from Skeletal Radiology, 2015; 44: 165-177)

The articular surfaces of the proximal metacarpal and distal trapezium form a saddle joint which allows for adduction/abduction, flexion/extension, and limited internal/external rotation (Figure 1.2). The basilar thumb joint has limited contribution to stability from bone geometry, so the

stability of the joint is supplemented by ligamentous and muscular actions. This allows for joint motion that can be used for a variety of functions.

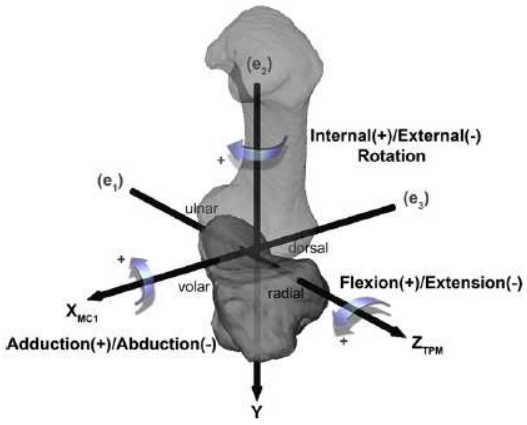

Figure 1.2 A representation of a simple coordinate system for the thumb basil joint (Used with permission from Journal of Biomechanics, 2013; 46: 1031-1034)

The proximal beak of the metacarpal is one of the basilar thumb joint's defining features and is thought to provide critical ligamentous attachment sites, and it is oriented volarly and medially. As many as sixteen ligaments have been identified to provide stability but the main two are the anterior oblique ligament (AOL), also known as the beak ligament or the deep anterior oblique ligament (dAOL), and the dorsoradial ligament (DRL) [2] (Figure 1.3).

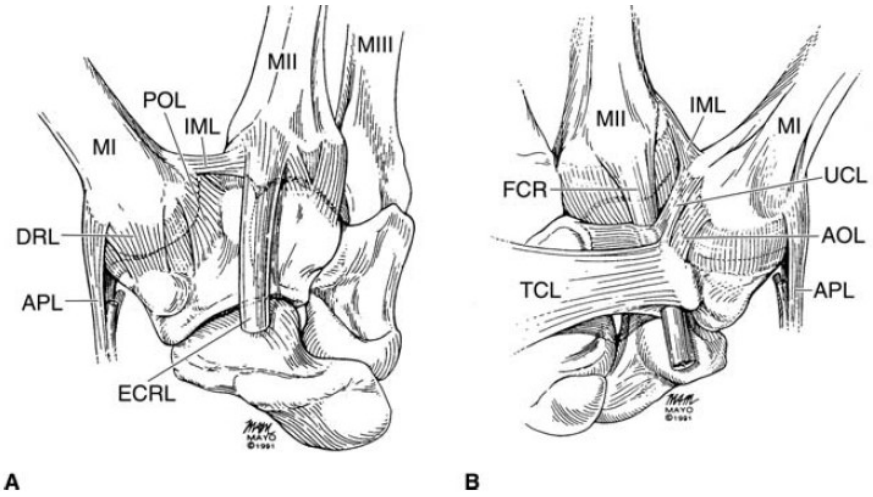

Figure 1.3 A – Dorsal view of the joint that shows the abductor pollicus longus (APL), dorsoradial ligament (DRL), posterior oblique ligament (POL), intermetacarpal ligament (IML), and the extensor carporadialis tendon (ECRL). B – Palmar view that shows the flexor carpi radialis (FCR), IML, ulnar collateral ligament (UCL), anterior oblique ligament (AOL), and APL. (Used with permission from Journal of American Academy of Orthopaedic Surgeons, 2008; 16: 140-151)

The AOL attaches to the volar beak of the metacarpal and at the volar side of the trapezium. The DRL attaches on the dorsoradial side of the metacarpal near the abductor pollicis longus (APL) insertion site and at the dorsoradial tubercle of the trapezium. There has been an ongoing debate over the exact roles of the AOL and the DRL in the joint's overall stability. Studies examining the contribution of each ligament towards its stability have used either anatomic or biomechanical analysis to arrive at their conclusions. The results of recent anatomical studies have generally come to the conclusion that the DRL contributes as much or more than the AOL to the joint's stability. Studies of mechanical properties of each ligament found that the stiffness [3, 4] and toughness [3] were significantly higher for the DRL than the AOL and that the DRL is the widest and thickest ligament in the joint [1, 2, 5, 6]. Studies of the other joints have shown that innervation of mechanoreceptors and nerve endings have an effect on its dynamic stability [7, 8]. Analysis of innervation patterns within the ligaments of the basilar thumb joint have concluded that there is a significantly greater distribution of nerve endings in the dorsal

ligaments than in the volar ligaments [9, 10]. A study performed by Bellinger et al to identify the TMC joint ligaments and their functions concluded that the AOL would prevent ulnar and volar subluxation and that the DRL prevented dorsal and dorsoradial subluxation [2]. However, a study by Doerschuk et al concluded that increased amounts of articular degeneration in the dorsal direction of the joint surface correlated with degeneration of the AOL [11]. Biomechanical studies using a combination of applied weights and serial sectioning of the joint's ligaments have drawn mixed conclusions that the DRL [12, 13] or the AOL [14] are the main prevention of dorsal displacement. Chenoweth et al performed a rotation shear test to characterize axial stability of the joint after sectioning the DRL, then sectioning the intermetacarpal ligament (IML), and finally a dorsoradial capsulodesis of the joint, and they concluded that axial laxity increased after transection of the DRL and IML with significantly decreased laxity after a capsulodesis repair [15]. Imaeda et al observed the recruitment patterns of the basilar thumb joint's ligaments during manual manipulation of cadaveric specimens and concluded that the AOL was a thick and broad ligament, and thus is the primary stabilizer of the thumb while the DRL likely provided little restriction to joint movement [16]. New anatomical and biomechanical studies have helped to increase the general knowledge surrounding the basilar thumb joint, but they have also created new questions as to what the exact roles of the AOL or the DRL are and which contributes more heavily to joint stability. It is likely that both play a substantial role in the overall stability of the joint.

Advances in computational modeling have led to additional studies focusing on analyzing changes in ligament tension in different anatomical positions. These studies included positioning the thumb in abduction/adduction, flexion/extension, or circumduction and other functional activities such as key pinch, jar grasp, and jar twist. While studies have agreed that each ligament

may provide greater support at different positions over the thumb's range of motion, they have differed on the exact role of each ligament. Contradictory findings of the AOL providing greater stabilization in abduction and extension [17, 18] and relatively lower tension in flexion, abduction, and opposition [19] have been reported. Halilaj et al stated that their findings suggested the AOL is slack over a large portion of the basilar thumb joint's range of motion [17]. Some agreement was found that the DRL provided greater stabilization in adduction [17, 18] and flexion [17, 19]. Studies assessing changes in ligament length during different functional tasks and motions are currently limited in number, so continued efforts to investigate this issue will help to reinforce or modify current knowledge about the role of each ligament.

1.2 Causes of Osteoarthritis and Diagnostic Procedures

Osteoarthritis (OA) can be a debilitating and painful condition that limits mobility of the joint and the daily functions of an individual. OA is defined as the degeneration of cartilage and the eventual exposure of subchondral bone (bone-on-bone contact). The subsequent bone-on-bone contact causes symptoms of pain, swelling, and inflammation. The basilar thumb joint is the second most affected joint within the hand [20]. Several studies have reported similar findings when analyzing portions of the population that are most likely affected by OA in the basilar thumb joint. A study in 2004 reported that OA of the basilar thumb joint affected 35.8% of their elderly study population [20]. Another study in 2006 reported that basilar thumb joint OA affected 17.7% and 21.0% of men and women, respectively, in their middle-aged and elderly study population [21]. Women are more commonly affected by OA in the basilar thumb joint than men [20, 21] and it occurs in approximately 33% of postmenopausal women [22]. The exact etiology of the disease has not been clearly defined, but both intrinsic and extrinsic factors have been thought to contribute to the OA's development. Hormonal differences with increasing age

lead to different cartilage material properties and ligamentous laxity, and these are thought to be primary causes leading to the development of OA [23, 24]. Shifts in contact locations are believed to be involved with the progression of OA as well. Anatomical studies and biomechanical studies of key pinch have shown that contact in the joint normally occurs in the volar region and that dorsal translation of contact location has been associated with increased articular wear, degeneration of the AOL, and the stage of OA [11, 25, 26] (Figure 1.4). Repeated shear forces in the volar region are thought to wear down the cartilage on the metacarpal and the AOL's attachment to the metacarpal beak, thus pressure shifts dorsally to areas that were originally unloaded [6, 25, 27]. Previous trauma to the bone, such as a Bennett fracture, or to the ligaments can also cause a shift in contact pressure that can lead to the development of OA [6, 28, 29].

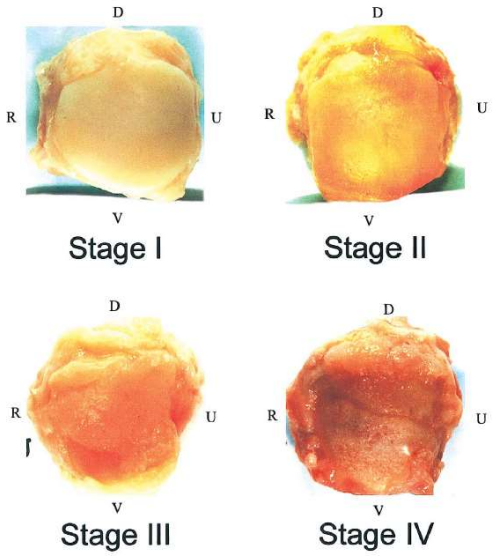

Figure 1.4 Progressive stages of osteoarthritis are correlated with increased articular wear on the volar portion of the joint (Used with permission from The Journal of Hand Surgery (American Ed.), 2003; 28: 597-604)

Current techniques for diagnosing OA in the basilar thumb joint involve a combination of a patient's history, physical examination, and radiographic examination. Pertinent patient

diagnostic factors for OA include the location, duration, frequency, level of pain, and activities that cause the pain to increase and decrease [30]. Physical examination includes checking for localized pain, swelling, and tenderness during palpation of the dorsal and dorsoradial aspects of the joint capsule as well as range of motion, loss of pinch strength, and laxity of the joint of the affected thumb compared to the contralateral [31]. Joint laxity and cartilage degradation that would lead to or indicate a diagnosis of OA can be confirmed and quantified radiographically. Several standard imaging views are regularly utilized to evaluate the condition of the joint and confirm the presence of OA. These views include anteroposterior (AP), also known as the posteroanterior (PA) or lateral view of the thumb, and oblique views. Positioning techniques, such as the Robert's view, Bett's view, and stress views, are often used to capture images specifically of the thumb and the basilar thumb joint (Figure 1.5).

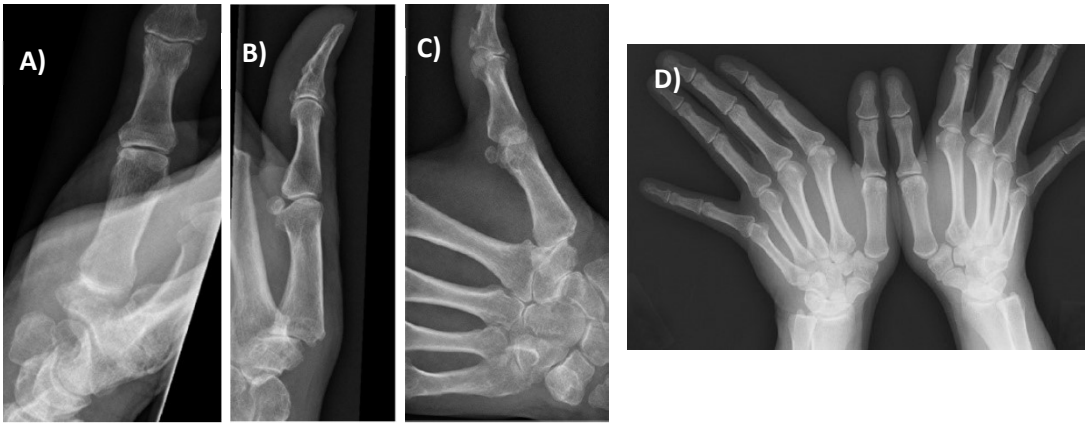

Figure 1.5 Various clinical views used to diagnose TMC pathology: A – Robert's view of the thumb carpometacarpal joint B – Lateral view of the thumb C – Bett's view of the thumb (Adapted from The Journal of Hand Surgery (American Ed.), 2011; 36: 1467-1470) D – Modified Eaton-Littler stress view (Adapted from The Journal of Hand Surgery (American Ed.), 2009; 34: 1402-1406)

The lateral view of the thumb is obtained by placing the palm flat against the X-ray plate. This is similar to a standard hand PA view. A PA or AP image of the hand does not provide a perfect lateral view of the basilar thumb joint, but it can provide a good approximation. These

approximate lateral views of the joint have been described as both PA or lateral (view of the thumb) in the literature which can create some confusion when attempting to compare results from different studies. The oblique view is obtained by initially placing the arm in a neutral rotation on the x-ray table and the forearm is then supinated 45 degrees. The PA view (or lateral view of the thumb) and oblique view tend to show substantial overlap between the metacarpals, trapezium, and trapezoid due to the orientation and shape of the metacarpal and trapezium, so other views of the basilar thumb joint have also been used to supplement them [32]. The Roberts view is obtained by hyperpronation of the forearm so that the dorsum of the thumb is flat on the x-ray plate to give a true AP view of the basilar thumb joint. This minimizes the overlap between the metacarpals, trapezium, and trapezoid. The Bett's view is obtained by pronation of the hand by 30º from a neutral forearm rotation and the imaging ray is angled 25º distally [33]. A Bett's view provides a true lateral view of the basilar thumb joint. The stress view was first suggested by Eaton and Littler to give a measure of the degree of laxity (or instability) of the joint, and it is obtained by taking an AP radiograph while the patient presses the radial sides of their thumbs together [28]. A combination of all these views are used as a tool in the diagnostic process to understand and grade the condition of the joint. The Eaton-Littler classification system is the most widely used grading scale for OA that is categorized into four stages [34] (Table 1.1). Joint space narrowing, increased subluxation, and the presence of joint debris are critical elements that are used to determine the stage of the disease. However, there is strong evidence showing that the inter-rater reliability between medical professionals using the system has been poor [34]. Radiographic examination of the hand can aide the diagnosis by eliminating other joints that may be painful and affected by arthritis. However, it should not be the only tool used to diagnose a patient, as symptomatic patients may show little radiographic evidence and asymptomatic

patients may have clear radiographic indications of OA [35]. All the information from patient history and examinations are used together to create a diagnosis for the joint because there is not one definitive sign that confirms an OA diagnosis.

Table 1.1 Eaton-Littler Classification Stages [28, 33]

Stage	Characteristics
I	In synovitis phase before development of significant capsule laxity. Small widening of the joint space (joint capsule distension). Less than 1/3 subluxation in any projection.
II	Significant capsular laxity with at least 1/3 subluxation in any projection. Small bone or calcified fragments less than 2 mm in diameter which are usually adjacent to volar or dorsal facets of trapezium
III	Greater than 1/3 subluxation. Fragments greater than 2 mm present in either or both dorsal or volar facets. Slight joint space narrowing.
IV	Advanced degenerative changes are present with major subluxation and very narrow joint space. Cystic and sclerotic subchondral bone changes are present. Margins of the trapezium show lipping and osteophyte formation. Significant erosion of the dorsoradial facet of the trapezium is present.

1.3 Treatment of Osteoarthritis in the Basilar Thumb Joint

Physical and radiographic evaluations are used to determine the stage of the disease, but the course of treatment is considerably driven by the severity of the patient's symptoms. The goal of treatment is to reduce pain and restore stability and function to the joint. Treatment options include both non-invasive conservative methods and invasive surgical procedures. Conservative treatments are initially used for Stage I and early Stage II OA. These treatments include hand therapy, splinting, and intra-articular injections. Studies that have looked at simple home exercises have used pain levels during active grip as indicators of improved or diminished hand function. They have reported conflicting results of either improvement [36, 37] or no improvement [38] when compared to control groups. The literature is not clear on a specific

recommended routine and provides various sets of exercises [36-40]. Exercise may also increase the dynamic stability of the joint which could reduce or delay the need for other pharmaceutical and surgical treatments [41, 42]. Splints are another simple treatment that has been used to provide additional support to the joint and relieve pain. Studies have shown splints are effective in reducing joint pain but they have differed on their effectiveness on improving dexterity, pinch strength, or grip strength when compared to control groups [43, 44]. Studies comparing prefabricated and custom splints showed that they produced similar results for pinch strength [44, 45] and that custom splints were better at reducing pain [44]. While supporting the joint with splints reduces pain, there is also a concern that prolonged use can cause muscle atrophy which can decrease hand strength [43]. If a splint is not effective on its own it can be used in combination with intra-articular injections to provide a greater benefit to the patient [46]. Corticosteroids and hyaluronic acid intra-articular injections have been used independently to treat basilar thumb joint OA. Both types of injections have benefits and potential drawbacks. Corticosteroids can effectively eliminate pain, but a potential drawback is weakening of the articular capsule and ligaments [47] which is thought to be an underlying causative factor in the development of OA. Hyaluronic acids are present in the synovial fluid joints and have been shown to exist in lower concentrations in osteoarthritic joints [48]. Injection of hyaluronic acids has been shown to restore some of the characteristic properties of synovial fluid and relieve joint pain [49], but a drawback to hyaluronic acids is multiple painful injections and their decreasing effectiveness over time [50]. Several studies have compared the effects of corticosteroid and hyaluronic acid injections and found similar results. Both injections significantly decreased pain in patients over a 6-12 month period with an increase in grip strength and either an increase in

pinch strength or no significant changes [47, 51, 52]. Studies differed on whether hyaluronic acid injections [52] or corticosteroid injections [51] provided more pain relief.

If more conservative methods of treatment are not effective in managing pain and symptoms, then surgical treatment may be considered. There are several factors that are taken into consideration before surgical intervention. The radiographic classification of OA, intensity of the joint pain, lifestyle, and failure of conservative treatments are all considered before surgery. Common procedures for early stage OA are volar ligament reconstruction, arthroscopic debridment, and metacarpal extension osteotomy. In a reconstruction of the volar ligament a tendon autograft, usually a portion of the flexor carpi radialis (FCR), is used to create a sling around the metacarpal that acts to recreate the stabilizing effect of the AOL and DRL (Figure 1.6). The radial half of the FCR is passed through a radial-ulnar hole drilled in the metacarpal base and passed under the abductor pollicus longus (APL) to simulate the DRL. It is then brought back radially around the joint and sutured to itself or the base of the metacarpal to simulate the AOL. Patients that underwent volar ligament reconstruction reported decreased pain in the joint and showed minimal progression of articular degeneration [28, 53]. However, patients still experienced some pain after the procedure, but it was much improved compared to the preoperative pain levels [53].

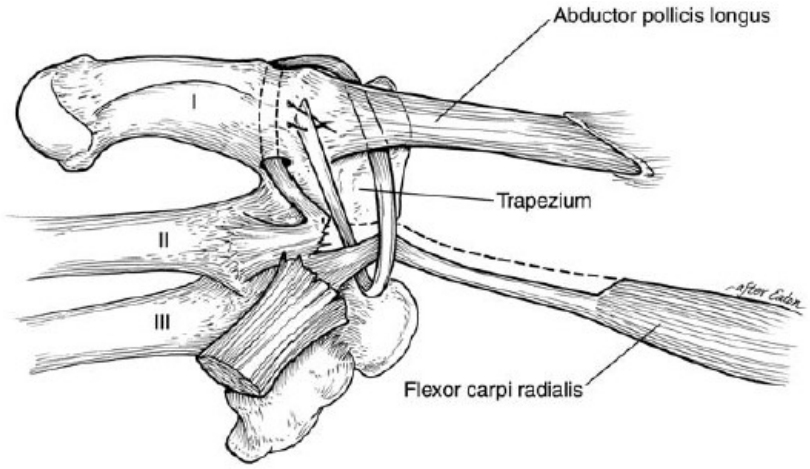

Figure 1.6 Reconstruction of the volar beak ligament (Used with permission from Journal of American Academy of Orthopaedic Surgeons, 2008; 16: 140-151)

Arthroscopic debridement of the joint is another less invasive option for early stage OA treatment (Figure 1.7). Small incisions are made above the basal joint for the insertion of an arthroscope and surgical resection tool to clear any loose segments of tissue and bone spurs. The requirement of only a few small incisions for the instruments leads to shorter recovery periods in patients [54]. Postoperative pain in the joint decreased when compared to preoperative levels [54, 55], but pain relief slowly diminished over time [55]. Studies have shown results of both higher pinch strength [54] and no change in pinch and grip strength [55].

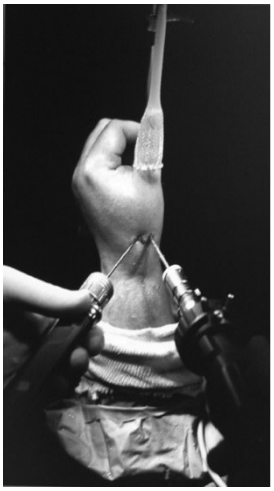

Figure 1.7 Surgical setup for arthroscopic debridement (Used with permission from Techniques in Hand and Upper Extremity Surgery, 2008; 12: 38-42)

Metacarpal osteotomy is a third surgical option available for early stage OA. A 15º-30º wedge of the metacarpal base is removed approximately one centimeter distal from the articular surface (Figure 1.8). This shifts the loading of the joint dorsally and away from the palmar compartment where osteoarthritic degeneration is thought to occur. Postoperative pain in the joint decreased [56, 57] while pinch strength either increased or remained the same when compared to contralateral [56, 57] or preoperative [58] values. Studies that compared preoperative and postoperative long-term radiographic progression of the disease showed either mixed results for disease progression [56, 57] or progression in a majority of the subjects [58].

Figure 1.8 A marked-up lateral radiograph for a planned osteotomy (Used with permission from The Journal of Hand Surgery (American Ed.), 2018; 43: 772.e1-772.e7)

In patients with more advanced OA surgical treatment is the main option. The gold standard for surgical treatments has been complete trapezium resection (Figure 1.9). Postoperative pain in the joint was has been reported to be lower than preoperative pain in patients [59, 60]. One of the concerns with complete trapeziectomy is a decrease in grip strength, and studies have reported results of both increases in pinch and grip strength when compared to preoperative values [60, 61] and decreases in strength when compared to contralateral values [59, 61].

Figure 1.9 PA radiograph of the hand illustrating simple trapeziectomy (Used with permission from The Journal of Hand Surgery (American Ed.), 2009; 34: 219-227)

Over time surgeons became concerned about possible instability resulting from the trapezial void, so other surgical treatments such as ligament reconstruction with trapeziectomy began to gain popularity to address the question of joint stability and the hole left behind by the resected trapezium. Trapeziectomy with ligament reconstruction and tendon interposition arthroplasty (LRTI) utilizes the radial portion of the FCR tendon to fill the void space of the resected trapezium (Figure 1.10). A hole is drilled in the metacarpal base and the FCR is passed through it in the ulnar to radial direction. The tendon tissue is sutured to itself and the surrounding metacarpal periosteum to create a sling that stabilizes the metacarpal base. The remaining tendon tissue is rolled up and sutured into the trapezial void to act as a spacer. Grip and pinch strength increased postoperatively, and postoperative pain levels decreased when compared to preoperative values [60-63].

Figure 1.10 Complete Trapeziectomy with Ligament Reconstruction and Tendon Interposition (LRTI) (Used with permission from Journal of American Academy of Orthopaedic Surgeons, 2008; 16: 140-151)

Studies that have compared complete trapeziectomy with and without ligament reconstruction have produced similar long-term results, so there has been no consensus as to which surgical

method is superior [60, 61]. Postoperative reduction in trapezium space was approximately 68% for trapeziectomy [60, 61] and ranged from 13% to 57% for LRTI [60, 61, 63, 64], but the difference in trapezial space reduction has not been shown to have a significant effect on postoperative pain or grip strength [60, 62-64]. Partial resection of the trapezium, also called hemitrapeziectomy, using arthroscopic debridement procedures has been viewed as another surgical option because it leaves ligamentous attachments between the base of the trapezium and the scaphoid intact to maintain some stability [65]. A similar surgical setup for arthroscopic debridement is used to gain access to the joint, and in addition to removing loose tissue and bone spurs the distal portion of the trapezium is resected (Figure 1.11). Postoperative pain levels decreased from preoperative values with either similar or increased pinch and grip strength [66-68]. Reduction in the trapezial space was between 4-15% [63, 67]. Other procedures such as tendon interposition or thermal capsular modification may be performed as well with a hemitrapeziectomy.

Figure 1.11 Fluoroscopic image of a hemitrapeziectomy (Used with permission from Arthroscopy, 2010; 26: 1395-1403)

Implant arthroplasty is another treatment option for more severe cases of basilar thumb joint OA, but implants have been associated with mixed results and high revision rates. A silicone implant was originally proposed by Swanson to fill the void left behind by trapezium resection and maintain thumb length [69] (Figure 1.12).

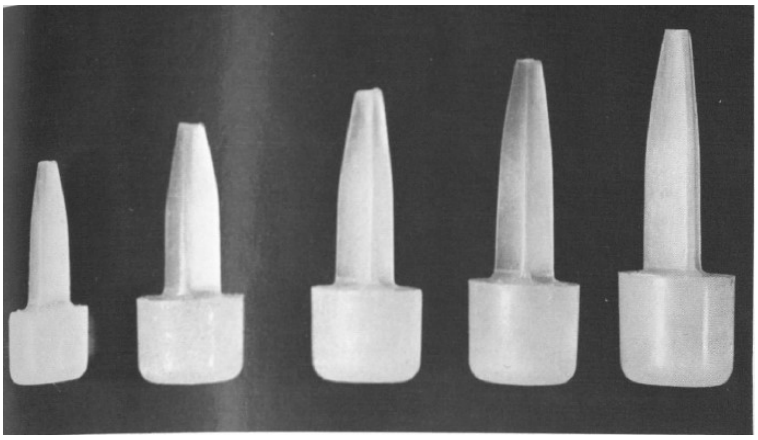

Figure 1.12 Swanson's intramedullary-stemmed silicone implant for total resection arthroplasty of the trapezium (Used with permission from The Journal of Bone and Joint Surgery (American Volume), 1972; 54: 456-471)

The entire trapezium was removed with care to prevent injuring the joint capsule. A canal was drilled into the metacarpal for the stem of the implant, and it was inserted so that the bottom of the implant was directly against the metacarpal base. Afterwards, the joint capsule was sutured back together (Figure 1.13). Issues with stability, implant debris, and synovitis caused by the implant caused it to lose popularity. A study in 2001 of 45 patients with a Swanson silicone implant found that 11 of the 45 had dislocated within 6 months of the surgery and found radiographic signs of silicone-induced synovitis in 5 patients as far out as 5 years after the primary surgery [70].

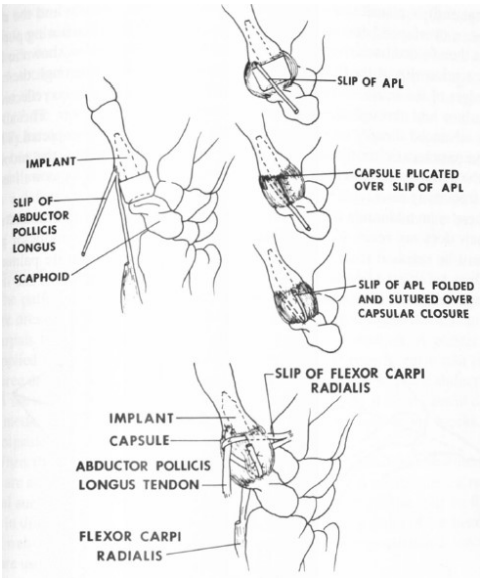

Figure 1.13 Insertion of the Swanson implant into the joint space (Used with permission from The Journal of Bone and Joint Surgery (American Volume), 1972; 54: 456-471)

Ball-and-socket designs followed Swanson's design with various degrees of success. Some of the current prosthetic implant designs include the Elektra, Motec, Moje, Maia, and ARPE. Implant designs such as the Elektra, Motec, and Moje have shown less successful long-term survival results and higher complication rates when compared to the Maia and ARPE implants (Figure 1.14).

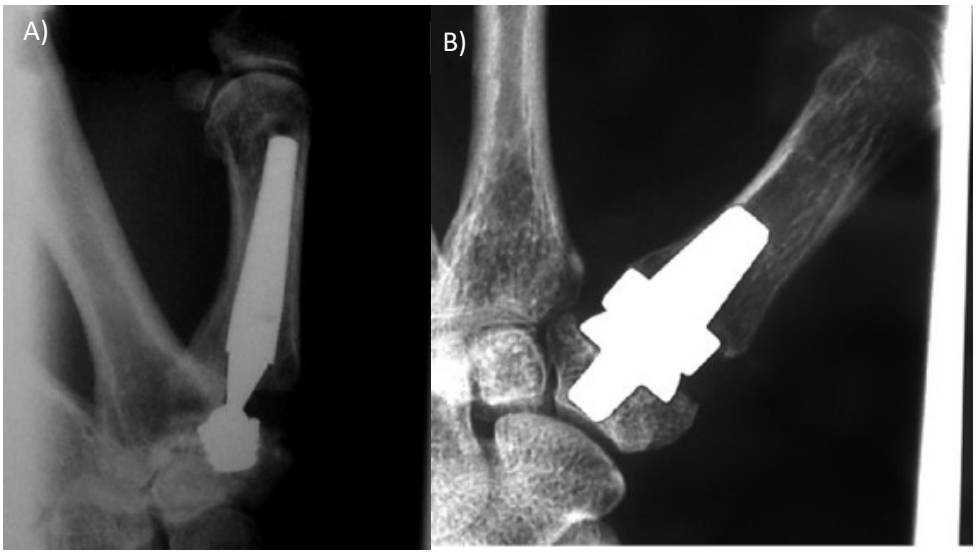

Figure 1.14 A – Elektra implant (Adapted from The Journal of Hand Surgery (American Ed.), 2013; 38: 863-871.e3). B – Moje implant (Adapted from The Journal of Hand Surgery (American Ed.), 2013; 38: 863-871.e3).

The Elektra implant consists of a threaded chrome-cobalt trapezium cup with a coat of hydroxyapatite (HA), a press-fit titanium metacarpal rod that is also coated with HA to increase osteointegration of the implant, and a ball and neck made with a metal-on-metal (MoM) chrome-cobalt steel articulation. Revision rates after a 10-13 month period for the Elektra implant were as high as 24% with the main cause of failure being aseptic loosening of the trapezium cup [71]. The Motec implant has a similar design as the Elektra implant, and it consists of a threaded metacarpal rod coated with Bonit R and a threaded trapezium cup with a MoM chrome-cobalt articulation. Revision rates were 42% after two years in one clinical study with the main cause of failure being aseptic loosening of the trapezium cup [72]. The Moje implant is a reverse ball and socket design that has joint interface surfaces lined with a glass-ceramic material called Bioverit to reduce friction, and the roughened surfaces on the metacarpal and trapezium stems are designed to improve osteointegration. In a clinical study with a mean follow-up of 33 months

(range of 9-62 months) performed by E. Kollig et al, 52% of the Moje implants had to be removed from patients due to failure caused by aseptic loosening [73].

Other prosthetic implants such as Maia and ARPE have had more success within 5 years after primary surgery (Figure 1.15). The Maia implant has a press-fit titanium alloy metacarpal rod and trapezium cup with a top layer of hydroxyapatite, a porous titanium lower layer, and a nitrogen steel head and neck. The revision rate in one clinical study, with a median follow-up of 76 months (range of 60-102 months), was 8.3% with the main complication being aseptic loosening of the trapezium cup [74]. Another study with the Maia implant reported complications, such as tenosynovitis, prosthetic dislocation, and trapezium cup loosening, in 56 out of 156 operations with 92.8% of those complications occurring within the first six months of surgery [75]. The ARPE implant has a press-fit titanium metacarpal rod and trapezium cup that are each coated with hydroxyapatite, and the neck is made from stainless steel. The complication rate in one clinical study, with a mean follow-up of 80 months, was 8.4% with the main complication being dislocation of the prosthesis head [76]. Dislocation of the prosthetic head and aseptic loosening of the trapezial base are commonly reported complications across different ball-and-socket implant designs [71-76]. These issues may be due to a ball-and-socket's inability to completely capture in vivo joint movement and kinematics. This could lead to overstresses that shorten the prosthetic's lifespan [77]. Increased research in the area of joint kinematics and motion of basilar thumb joints after implant arthroplasty could increase the lifespan of prosthetics and make them a more desirable treatment option.

Figure 1.15 A – Maia implant (Adapted from The Journal of Hand Surgery (American Ed.), 2017; 42: 838.e1-838.e8). B – ARPE implant (Adapted from The Journal of Hand Surgery (American Ed.), 2017; 42: 630-638).

The choice of surgical procedure performed for advanced arthritis is influenced by the surgeon's preference and experience. A review by Yuan et al. showed that 89.3% of patients in the United States in 2010 who were 65 years of age or older underwent total or partial trapeziectomy with LRTI, 5.1% underwent simple trapeziectomy, and 5.6% underwent CMC arthrodesis or prosthetic arthroplasty [78]. The vast majority of surgeons (93%) performed only one type of procedure with the majority performing complete or partial trapeziectomy with LRTI [78]. Concerns over joint instability in complete trapeziectomy drove innovation that led to more complicated procedures such as LRTI, partial trapeziectomy, and prosthetic arthroplasty but studies have shown that they produce similar results in terms of pain and patient satisfaction. This has led some surgeons to prefer simpler techniques over the use of more advanced surgical techniques or prosthetics. The variability in prosthetic success is likely another contributing reason as to why very few surgeons in the United States perform basilar thumb joint implant arthroplasty.

1.4 The Use of Finite Element Analysis for Joint Contact Analysis

Finite element analysis has previously been used to research joint contact mechanics [79-82]. It can be used as a tool to study in vivo contact pressure patterns and measures of contact mechanics within joints while avoiding disruption of the ligaments and soft tissues that contribute to their stability. Model geometries and kinematics can also be defined for specimen or subject-specific scenarios. This would eliminate some of the assumptions made during geometry creation and application of boundary conditions. Subject-specific models could potentially be used to drive clinical research aims, develop effective diagnostic and therapeutic techniques, understand what drives differences in joint mechanobiology in men and women, and how that leads to OA. Before finite element models can be used with confidence, they must first be validated against experimental data to provide evidence that the modeling process will provide accurate predictions.

1.5 Research Objectives

The current research was driven by two objectives. The first objective was focused on defining a radiographic imaging technique that can be used to aide research and diagnosis of OA in the basilar thumb joint. While the stress view radiograph [28], as previously defined by Eaton and Littler, allows for visualizing and quantifying subluxation, it has not been correlated with disease and/or abnormal joint mechanics during functional tasks [83]. Thus, it was our goal to develop a radiographic technique to measure lateral subluxation during the functional task of active key pinch. This method yields a measure of poor joint mechanics if radiographic and visual OA grades correlate to subluxation of the metacarpal within the basilar thumb joint, and it can then provide a simple diagnostic technique and consistent view to measure metacarpal lateral subluxation in clinical settings. Wide spread use of a consistent measure would allow results

from different studies to be more directly compared and would give physicians another tool to aide them in evaluating OA risk. For this study, specimens simulating key pinch were radiographed from 0º (standard AP view) with the top of a C-arm rotated by 5º increments towards the ulnar aspect of the arm up to 60º. This effectively simulated supination of the hand in the AP view. Lateral subluxation of the metacarpal base was measured to determine which imaging angle would provide the best and most complete view of subluxation. We also evaluated the role of the AOL in preventing lateral subluxation with two additional sets of radiographs. The second image set was taken after the joint capsule was opened, and the third was taken after the AOL was transected. The second objective was focused on a finite element modeling technique for analysis of contact mechanics in the basilar thumb joint. A direct validation study for a finite element modeling technique was conducted using MRI images from a clinical scanner to create finite element models, and the results were compared to cadaveric experimental data recorded using an electronic K-Scan^{TM} Wrist Sensor #4201 (Tekscan Inc., South Boston, MA, USA) during simulated lateral pinch. Average contact pressure, peak contact pressure, contact area, and contact force from the model were compared to the experimental Tekscan data using a set validation criterion.

1.6 References

1. Edmunds, J.O., *Current concepts of the anatomy of the thumb trapeziometacarpal joint.* J Hand Surg Am, 2011. **36**(1): p. 170-82.
2. Bettinger, P.C., R.L. Linscheid, R.A. Berger, W.P. Cooney, 3rd, and K.N. An, *An anatomic study of the stabilizing ligaments of the trapezium and trapeziometacarpal joint.* J Hand Surg Am, 1999. **24**(4): p. 786-98.

3. Bettinger, P.C., W.P. Smutz, R.L. Linscheid, W.P. Cooney, 3rd, and K.N. An, *Material properties of the trapezial and trapeziometacarpal ligaments.* J Hand Surg Am, 2000. **25**(6): p. 1085-95.

4. D'Agostino, P., F.D. Kerkhof, M. Shahabpour, J.P. Moermans, F. Stockmans, and E.E. Vereecke, *Comparison of the anatomical dimensions and mechanical properties of the dorsoradial and anterior oblique ligaments of the trapeziometacarpal joint.* J Hand Surg Am, 2014. **39**(6): p. 1098-107.

5. Colman, M., D.P. Mass, and L.F. Draganich, *Effects of the deep anterior oblique and dorsoradial ligaments on trapeziometacarpal joint stability.* J Hand Surg Am, 2007. **32**(3): p. 310-7.

6. Melville, D.M., M.S. Taljanovic, L.R. Scalcione, J.M. Eble, L.H. Gimber, G.L. DeSilva, and J.E. Sheppard, *Imaging and management of thumb carpometacarpal joint osteoarthritis.* Skeletal Radiol, 2015. **44**(2): p. 165-77.

7. Johansson, H., P. Sjolander, and P. Sojka, *A sensory role for the cruciate ligaments.* Clin Orthop Relat Res, 1991(268): p. 161-78.

8. Hagert, E., M. Garcia-Elias, S. Forsgren, and B.O. Ljung, *Immunohistochemical analysis of wrist ligament innervation in relation to their structural composition.* J Hand Surg Am, 2007. **32**(1): p. 30-6.

9. Hagert, E., J. Lee, and A.L. Ladd, *Innervation patterns of thumb trapeziometacarpal joint ligaments.* J Hand Surg Am, 2012. **37**(4): p. 706-714.e1.

10. Ladd, A.L., J. Lee, and E. Hagert, *Macroscopic and microscopic analysis of the thumb carpometacarpal ligaments: a cadaveric study of ligament anatomy and histology.* J Bone Joint Surg Am, 2012. **94**(16): p. 1468-77.

11. Doerschuk, S.H., D.G. Hicks, V.M. Chinchilli, and V.D. Pellegrini, Jr., *Histopathology of the palmar beak ligament in trapeziometacarpal osteoarthritis.* J Hand Surg Am, 1999. **24**(3): p. 496-504.

12. Strauch, R.J., M.J. Behrman, and M.P. Rosenwasser, *Acute dislocation of the carpometacarpal joint of the thumb: an anatomic and cadaver study.* J Hand Surg Am, 1994. **19**(1): p. 93-8.

13. Van Brenk, B., R.R. Richards, M.B. Mackay, and E.L. Boynton, *A biomechanical assessment of ligaments preventing dorsoradial subluxation of the trapeziometacarpal joint.* J Hand Surg Am, 1998. **23**(4): p. 607-11.

14. Imaeda, T., G. Niebur, K.N. An, and W.P. Cooney, 3rd, *Kinematics of the trapeziometacarpal joint after sectioning of ligaments.* J Orthop Res, 1994. **12**(2): p. 205-10.

15. Chenoweth, B.A., G.D. O'Mahony, C. Fitzgerald, J.A. Stoner, D.L. O'Donoghue, and G.M. Rayan, *Efficacy of Dorsoradial Capsulodesis for Trapeziometacarpal Joint Instability: A Cadaver Study.* J Hand Surg Am, 2017. **42**(1): p. e25-e31.

16. Imaeda, T., K.N. An, W.P. Cooney, 3rd, and R. Linscheid, *Anatomy of trapeziometacarpal ligaments.* J Hand Surg Am, 1993. **18**(2): p. 226-31.

17. Halilaj, E., M.J. Rainbow, D.C. Moore, D.H. Laidlaw, A.P. Weiss, A.L. Ladd, and J.J. Crisco, *In vivo recruitment patterns in the anterior oblique and dorsoradial ligaments of the first carpometacarpal joint.* J Biomech, 2015. **48**(10): p. 1893-8.

18. Imaeda, T., G. Niebur, W.P. Cooney, R.L. Linscheid, and K.-N. An, *Ligament length during circumduction of the trapeziometacarpal joint.* Journal of orthopaedic science, 1997. **2**(5): p. 319-327.

19. Tan, J., J. Xu, R.G. Xie, A.D. Deng, and J.B. Tang, *In vivo length and changes of ligaments stabilizing the thumb carpometacarpal joint.* J Hand Surg Am, 2011. **36**(3): p. 420-7.

20. Dahaghin, S., S.M. Bierma-Zeinstra, A.Z. Ginai, H.A. Pols, J.M. Hazes, and B.W. Koes, *Prevalence and pattern of radiographic hand osteoarthritis and association with pain and disability (the Rotterdam study).* Ann Rheum Dis, 2005. **64**(5): p. 682-7.

21. Wilder, F.V., J.P. Barrett, and E.J. Farina, *Joint-specific prevalence of osteoarthritis of the hand.* Osteoarthritis Cartilage, 2006. **14**(9): p. 953-7.

22. Armstrong, A.L., J.B. Hunter, and T.R. Davis, *The prevalence of degenerative arthritis of the base of the thumb in post-menopausal women.* J Hand Surg Br, 1994. **19**(3): p. 340-1.

23. Van Heest, A.E. and P. Kallemeier, *Thumb carpal metacarpal arthritis.* J Am Acad Orthop Surg, 2008. **16**(3): p. 140-51.

24. Ladd, A.L., A.P. Weiss, J.J. Crisco, E. Hagert, J.M. Wolf, S.Z. Glickel, and J. Yao, *The thumb carpometacarpal joint: anatomy, hormones, and biomechanics.* Instr Course Lect, 2013. **62**: p. 165-79.

25. Pellegrini, V.D., Jr., C.W. Olcott, and G. Hollenberg, *Contact patterns in the trapeziometacarpal joint: the role of the palmar beak ligament.* J Hand Surg Am, 1993. **18**(2): p. 238-44.

26. Koff, M.F., O.F. Ugwonali, R.J. Strauch, M.P. Rosenwasser, G.A. Ateshian, and V.C. Mow, *Sequential wear patterns of the articular cartilage of the thumb carpometacarpal joint in osteoarthritis.* J Hand Surg Am, 2003. **28**(4): p. 597-604.

27. Moulton, M.J., M.A. Parentis, M.J. Kelly, C. Jacobs, S.H. Naidu, and V.D. Pellegrini, Jr., *Influence of metacarpophalangeal joint position on basal joint-loading in the thumb.* J Bone Joint Surg Am, 2001. **83-a**(5): p. 709-16.

28. Eaton, R.G. and J.W. Littler, *Ligament reconstruction for the painful thumb carpometacarpal joint.* J Bone Joint Surg Am, 1973. **55**(8): p. 1655-66.

29. Cullen, J.P., M.A. Parentis, V.M. Chinchilli, and V.D. Pellegrini, Jr., *Simulated Bennett fracture treated with closed reduction and percutaneous pinning. A biomechanical analysis of residual incongruity of the joint.* J Bone Joint Surg Am, 1997. **79**(3): p. 413-20.

30. Patel, T.J., P.K. Beredjiklian, and J.L. Matzon, *Trapeziometacarpal joint arthritis.* Curr Rev Musculoskelet Med, 2013. **6**(1): p. 1-8.

31. Barron, O.A., S.Z. Glickel, and R.G. Eaton, *Basal joint arthritis of the thumb.* J Am Acad Orthop Surg, 2000. **8**(5): p. 314-23.

32. Oheb, J., Y. Lansinger, J.A. Jansen, J.Q. Nguyen, M.A. Porembski, and G.M. Rayan, *Radiographic Assessment of the Robert and Lateral Views in Trapeziometacarpal Osteoarthrosis.* Hand Surg, 2015. **20**(2): p. 251-9.

33. Billing, L. and K.-O. Gedda, *Roentgen examination of Bennett's fracture.* Acta radiologica, 1952(6): p. 471-476.

34. Berger, A.J., A. Momeni, and A.L. Ladd, *Intra- and interobserver reliability of the Eaton classification for trapeziometacarpal arthritis: a systematic review.* Clin Orthop Relat Res, 2014. **472**(4): p. 1155-9.

35. Brown, G.D., 3rd, M.S. Roh, R.J. Strauch, M.P. Rosenwasser, G.A. Ateshian, and V.C. Mow, *Radiography and visual pathology of the osteoarthritic scaphotrapezio-trapezoidal*

joint, and its relationship to trapeziometacarpal osteoarthritis. J Hand Surg Am, 2003. **28**(5): p. 739-43.

36. Stamm, T.A., K.P. Machold, J.S. Smolen, S. Fischer, K. Redlich, W. Graninger, W. Ebner, and L. Erlacher, *Joint protection and home hand exercises improve hand function in patients with hand osteoarthritis: a randomized controlled trial.* Arthritis Rheum, 2002. **47**(1): p. 44-9.
37. Rogers, M.W. and F.V. Wilder, *The effects of strength training among persons with hand osteoarthritis: a two-year follow-up study.* J Hand Ther, 2007. **20**(3): p. 244-9; quiz 250.
38. Rogers, M.W. and F.V. Wilder, *Exercise and hand osteoarthritis symptomatology: a controlled crossover trial.* J Hand Ther, 2009. **22**(1): p. 10-7; discussion 19-20; quiz 18.
39. Valdes, K. and R. von der Heyde, *An exercise program for carpometacarpal osteoarthritis based on biomechanical principles.* J Hand Ther, 2012. **25**(3): p. 251-62; quiz 263.
40. DeMott, L., *Novel isometric exercises for the dynamic stability programs for thumb carpal metacarpal joint instability.* J Hand Ther, 2017. **30**(3): p. 372-375.
41. Poole, J.U. and V.D. Pellegrini, Jr., *Arthritis of the thumb basal joint complex.* J Hand Ther, 2000. **13**(2): p. 91-107.
42. Taylor, J., *Restoration of dynamic stability in early osteoarthritis of the carpometacarpal joint of the thumb.* The British Journal of Hand Therapy, 2000. **5**(2): p. 37-41.
43. Gomes Carreira, A.C., A. Jones, and J. Natour, *Assessment of the effectiveness of a functional splint for osteoarthritis of the trapeziometacarpal joint on the dominant hand: a randomized controlled study.* J Rehabil Med, 2010. **42**(5): p. 469-74.

44. Bani, M.A., M. Arazpour, R.V. Kashani, M.E. Mousavi, and S.W. Hutchins, *Comparison of custom-made and prefabricated neoprene splinting in patients with the first carpometacarpal joint osteoarthritis.* Disabil Rehabil Assist Technol, 2013. **8**(3): p. 232-7.

45. Grenier, M.L., R. Mendonca, and P. Dalley, *The effectiveness of orthoses in the conservative management of thumb CMC joint osteoarthritis: An analysis of functional pinch strength.* J Hand Ther, 2016. **29**(3): p. 307-13.

46. Day, C.S., R. Gelberman, A.A. Patel, M.T. Vogt, K. Ditsios, and M.I. Boyer, *Basal joint osteoarthritis of the thumb: a prospective trial of steroid injection and splinting.* J Hand Surg Am, 2004. **29**(2): p. 247-51.

47. Stahl, S., I. Karsh-Zafrir, N. Ratzon, and N. Rosenberg, *Comparison of intraarticular injection of depot corticosteroid and hyaluronic acid for treatment of degenerative trapeziometacarpal joints.* J Clin Rheumatol, 2005. **11**(6): p. 299-302.

48. Adams, M.E., A.J. Lussier, and J.G. Peyron, *A risk-benefit assessment of injections of hyaluronan and its derivatives in the treatment of osteoarthritis of the knee.* Drug Saf, 2000. **23**(2): p. 115-30.

49. Ghosh, P. and D. Guidolin, *Potential mechanism of action of intra-articular hyaluronan therapy in osteoarthritis: are the effects molecular weight dependent?* Semin Arthritis Rheum, 2002. **32**(1): p. 10-37.

50. Karalezli, N., T.C. Ogun, S. Kartal, S.N. Saracgil, M. Yel, and I. Tuncay, *The pain associated with intraarticular hyaluronic acid injections for trapeziometacarpal osteoarthritis.* Clin Rheumatol, 2007. **26**(4): p. 569-71.

51. Bahadir, C., B. Onal, V.Y. Dayan, and N. Gurer, *Comparison of therapeutic effects of sodium hyaluronate and corticosteroid injections on trapeziometacarpal joint osteoarthritis.* Clin Rheumatol, 2009. **28**(5): p. 529-33.

52. Fuchs, S., R. Monikes, A. Wohlmeiner, and T. Heyse, *Intra-articular hyaluronic acid compared with corticoid injections for the treatment of rhizarthrosis.* Osteoarthritis Cartilage, 2006. **14**(1): p. 82-8.

53. Freedman, D.M., R.G. Eaton, and S.Z. Glickel, *Long-term results of volar ligament reconstruction for symptomatic basal joint laxity.* J Hand Surg Am, 2000. **25**(2): p. 297-304.

54. Furia, J.P., *Arthroscopic debridement and synovectomy for treating basal joint arthritis.* Arthroscopy, 2010. **26**(1): p. 34-40.

55. Wong, C.W. and P.C. Ho, *Arthroscopic Management of Thumb Carpometacarpal Joint Arthritis.* Hand Clin, 2017. **33**(4): p. 795-812.

56. Chou, F.H., J.J. Irrgang, and R.J. Goitz, *Long-term follow-up of first metacarpal extension osteotomy for early CMC arthritis.* Hand (N Y), 2014. **9**(4): p. 478-83.

57. Parker, W.L., R.L. Linscheid, and P.C. Amadio, *Long-term outcomes of first metacarpal extension osteotomy in the treatment of carpal-metacarpal osteoarthritis.* J Hand Surg Am, 2008. **33**(10): p. 1737-43.

58. Bachoura, A., E.J. Yakish, and J.D. Lubahn, *Survival and Long-Term Outcomes of Thumb Metacarpal Extension Osteotomy for Symptomatic Carpometacarpal Laxity and Early Basal Joint Arthritis.* J Hand Surg Am, 2018.

59. Elvebakk, K., I.E. Johnsen, C.B. Wold, T. Finsen, H. Russwurm, and V. Finsen, *Simple Trapeziectomy for Arthrosis of the Basal Joint of the Thumb: 49 Thumbs Reviewed After Two Years.* Hand Surg, 2015. **20**(3): p. 435-9.

60. Field, J. and D. Buchanan, *To suspend or not to suspend: a randomised single blind trial of simple trapeziectomy versus trapeziectomy and flexor carpi radialis suspension.* J Hand Surg Eur Vol, 2007. **32**(4): p. 462-6.

61. De Smet, L., W. Sioen, D. Spaepen, and H. van Ransbeeck, *Treatment of basal joint arthritis of the thumb: trapeziectomy with or without tendon interposition/ligament reconstruction.* Hand Surg, 2004. **9**(1): p. 5-9.

62. Lins, R.E., R.H. Gelberman, L. McKeown, J.N. Katz, and R.K. Kadiyala, *Basal joint arthritis: trapeziectomy with ligament reconstruction and tendon interposition arthroplasty.* J Hand Surg Am, 1996. **21**(2): p. 202-9.

63. Tomaino, M.M., V.D. Pellegrini, Jr., and R.I. Burton, *Arthroplasty of the basal joint of the thumb. Long-term follow-up after ligament reconstruction with tendon interposition.* J Bone Joint Surg Am, 1995. **77**(3): p. 346-55.

64. Reissner, L., M. Marks, S. Schindele, and D.B. Herren, *Comparison of clinical outcome with radiological findings after trapeziectomy with ligament reconstruction and tendon interposition.* J Hand Surg Eur Vol, 2016. **41**(3): p. 335-9.

65. Hentz, V.R., *Surgical treatment of trapeziometacarpal joint arthritis: a historical perspective.* Clin Orthop Relat Res, 2014. **472**(4): p. 1184-9.

66. Earp, B.E., A.C. Leung, P.E. Blazar, and B.P. Simmons, *Arthroscopic hemitrapeziectomy with tendon interposition for arthritis at the first carpometacarpal joint.* Tech Hand Up Extrem Surg, 2008. **12**(1): p. 38-42.

67. Edwards, S.G. and P.N. Ramsey, *Prospective outcomes of stage III thumb carpometacarpal arthritis treated with arthroscopic hemitrapeziectomy and thermal capsular modification without interposition.* J Hand Surg Am, 2010. **35**(4): p. 566-71.

68. Hofmeister, E.P., R.S. Leak, R.W. Culp, and A.L. Osterman, *Arthroscopic hemitrapeziectomy for first carpometacarpal arthritis: results at 7-year follow-up.* Hand (N Y), 2009. **4**(1): p. 24-8.

69. Swanson, A.B., *Disabling arthritis at the base of the thumb: treatment by resection of the trapezium and flexible (silicone) implant arthroplasty.* J Bone Joint Surg Am, 1972. **54**(3): p. 456-71.

70. van Cappelle, H.G., R. Deutman, and J.R. van Horn, *Use of the Swanson silicone trapezium implant for treatment of primary osteoarthritis : long-term results.* J Bone Joint Surg Am, 2001. **83-a**(7): p. 999-1004.

71. Hansen, T.B. and L. Snerum, *Elektra trapeziometacarpal prosthesis for treatment of osteoarthrosis of the basal joint of the thumb.* Scand J Plast Reconstr Surg Hand Surg, 2008. **42**(6): p. 316-9.

72. Thillemann, J.K., T.M. Thillemann, B. Munk, and K. Kroner, *High revision rates with the metal-on-metal Motec carpometacarpal joint prosthesis.* J Hand Surg Eur Vol, 2016. **41**(3): p. 322-7.

73. Kollig, E., W. Weber, D. Bieler, and A. Franke, *Failure of an uncemented thumb carpometacarpal joint ceramic prosthesis.* J Hand Surg Eur Vol, 2017. **42**(6): p. 599-604.

74. Toffoli, A. and J. Teissier, *MAIA Trapeziometacarpal Joint Arthroplasty: Clinical and Radiological Outcomes of 80 Patients With More than 6 Years of Follow-Up.* J Hand Surg Am, 2017. **42**(10): p. 838.e1-838.e8.

75. Bricout, M. and J. Rezzouk, *Complications and failures of the trapeziometacarpal Maia((R)) prosthesis: A series of 156 cases.* Hand Surg Rehabil, 2016. **35**(3): p. 190-198.

76. Cootjans, K., J. Vanhaecke, M. Dezillie, J. Barth, H. Pottel, and F. Stockmans, *Joint Survival Analysis and Clinical Outcome of Total Joint Arthroplasties With the ARPE Implant in the Treatment of Trapeziometacarpal Osteoarthritis With a Minimal Follow-Up of 5 Years.* J Hand Surg Am, 2017. **42**(8): p. 630-638.

77. Spartacus, V., A. Mayoly, A. Gay, T. Le Corroller, M. Nemoz-Gaillard, S. Roffino, and P. Chabrand, *Biomechanical causes of trapeziometacarpal arthroplasty failure.* Comput Methods Biomech Biomed Engin, 2017. **20**(11): p. 1233-1235.

78. Yuan, F., O. Aliu, K.C. Chung, and E. Mahmoudi, *Evidence-Based Practice in the Surgical Treatment of Thumb Carpometacarpal Joint Arthritis.* J Hand Surg Am, 2017. **42**(2): p. 104-112.e1.

79. Schneider, M.T.Y., J. Zhang, J.J. Crisco, A.C. Weiss, A.L. Ladd, K. Mithraratne, P. Nielsen, and T. Besier, *Trapeziometacarpal joint contact varies between men and women during three isometric functional tasks.* Med Eng Phys, 2017. **50**: p. 43-49.

80. Johnson, J.E., P. Lee, T.E. McIff, E.B. Toby, and K.J. Fischer, *Computationally efficient magnetic resonance imaging based surface contact modeling as a tool to evaluate joint injuries and outcomes of surgical interventions compared to finite element modeling.* J Biomech Eng, 2014. **136**(4).

81. Henak, C.R., E.D. Carruth, A.E. Anderson, M.D. Harris, B.J. Ellis, C.L. Peters, and J.A. Weiss, *Finite element predictions of cartilage contact mechanics in hips with retroverted acetabula.* Osteoarthritis Cartilage, 2013. **21**(10): p. 1522-9.

82. Akbarshahi, M., J.W. Fernandez, A.G. Schache, and M.G. Pandy, *Subject-specific evaluation of patellofemoral joint biomechanics during functional activity.* Med Eng Phys, 2014. **36**(9): p. 1122-33.

83. Halilaj, E., D.C. Moore, T.K. Patel, A.L. Ladd, A.P. Weiss, and J.J. Crisco, *Early osteoarthritis of the trapeziometacarpal joint is not associated with joint instability during typical isometric loading.* J Orthop Res, 2015. **33**(11): p. 1639-45.

Chapter 2. Dorsal Subluxation of the Metacarpal in the Basilar Thumb Joint during Key Pinch and its Correlation to Osteoarthritic Grades

2.1 Abstract

The basilar thumb joint is the joint second most commonly affected by osteoarthritis (OA) in the hand. Radiographic analysis of the joint using the Eaton-Littler grading system is commonly used by physicians as a tool to assess OA risk and aid diagnosis. Also, stress radiographs using functional tasks, such as key pinch, can be used to evaluate the instability of the joint. Laxity of the anterior oblique ligament (AOL) and the dorsoradial ligament (DRL) are believed to contribute to the progression of OA through increased dorsal subluxation. Eleven cadaveric specimens were rigged to simulate key pinch, and anteroposterior (AP) radiographs were recorded with a mobile C-arm. To capture the series of images, the top of the C-arm was rotated at 5º increments toward the ulnar aspect of the arm up to 60º to determine the best view for evaluating the maximum subluxation. The AP view showed the maximum amount of subluxation in a majority of the specimens. Subluxation for the intact joint capsules were compared to Eaton-Littler radiographic classifications, the Outerbridge classification, and the International Cartilage Repair Society (ICRS) visual classification for OA. Subluxation was only significantly correlated to the Eaton-Littler grades. These results indicate that key pinch stress radiographs could be a useful tool to supplement radiographic grading. The effects of sectioning the joint capsule and the AOL on subluxation were measured during key pinch, and neither had a statistically significant effect on the amount of subluxation. This supports more recent studies that argue the AOL plays a smaller role in preventing dorsal subluxation.

2.2 Introduction

The basilar thumb joint, also known as the thumb carpometacarpal (CMC) joint or the trapeziometacarpal (TMC) joint, is the second most common joint of the hand to be affected by osteoarthritis (OA) [1, 2]. Radiographic images are commonly used as a tool to aide in diagnosing OA. The oblique orientation of the joint and the curvature of its surfaces cause overlaps between the trapezium, trapezoid, and first and second metacarpals in some standard imaging views, so a combination of these views is often used to visualize the condition of the joint (Figure 2.1). The standard imaging views used for radiographic evaluation of the hand are posteroanterior (PA) or anteroposterior (AP), lateral, and oblique. One of those views, a PA radiograph of the hand, can be used to get an approximate lateral view of the basilar thumb joint (Figure 2.1B). Different positioning techniques are often used specifically to image the thumb. A true AP view of the thumb, also called the Robert's view, provides a dorsal view of the joint that minimizes the overlap between the first and second metacarpals, trapezium, and trapezoid (Figure 2.1A). Another view which provides a true lateral view of the thumb, also called the Bett's view, is obtained by pronation of the hand by 30º from a neutral forearm rotation and the imaging ray angled 25º distally (Figure 2.1C) [3]. Both basic views of the hand and specific views of the thumb have been used for radiographic analysis of the basilar thumb joint.

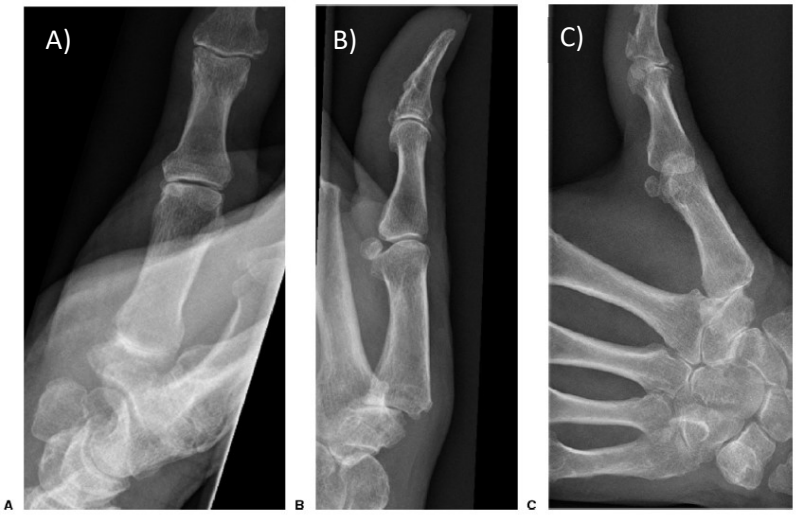

Figure 2.1 Various clinical views used to diagnose TMC pathology: A – Robert's view of the thumb carpometacarpal joint B – Lateral view of the thumb C – Bett's view of the thumb (Adapted from The Journal of Hand Surgery (American Ed.), 2011; 36: 1467-1470)

Instability of the joint has been believed to be a factor in the development and progression of OA [4, 5]. Stress view radiographs are a tool that can be used in clinical settings to evaluate the joint stability by quantifying the amount of lateral subluxation of the metacarpal (Figure 2.2). Eaton and Littler first suggested a stress view radiograph in 1973 to directly characterize the laxity (instability) of the stabilizing ligaments for the joint by measuring metacarpal lateral subluxation [4]. They defined the stress radiograph as a PA view with the patient's arms flat on the image receptor and the radial portions of the thumbs pressed together. A modified version of Eaton and Littler's stress radiograph was suggested by Wolf et al., and they reported high inter-rater reliability using their modified technique [6, 7]. Stress view radiographs are diagnostically used to confirm the general joint stability that physicians observe during physical examinations.

Figure 2.2 Modified Eaton-Littler stress view proposed by Wolf et al. to quantify radial (lateral) subluxation (Adapted from The Journal of Hand Surgery (American Ed.), 2009; 34: 1402-1406)

A stress view radiograph taken during key pinch has been used to evaluate the change in basal joint height after various reconstructive surgeries [8], and key pinch has been used in additional ways as a clinical and diagnostic tool. A reduction in grip strength during key pinch strength has been correlated with the presence of OA in the thumb basil joint [9, 10]. A recent study published by Halilaj et al reported that the basilar thumb joint experienced greater instability during key pinch than other functional tasks such as jar grasp and jar twist [11]. This suggests that key pinch stress radiographs may have other potential clinical applications, such as assessing stability (i.e. lateral subluxation of the metacarpal) of the basilar thumb joint. To our knowledge there have not been any studies on the degree of joint stability during a key pinch and its relation to OA severity.

Studies within the literature have used various imaging techniques designed for both the hand and the thumb to examine the basilar thumb joint [7, 12-15]. Eaton and Littler proposed a four-stage radiographic classification system for OA diagnosis in the basilar thumb joint in 1973 (Figure 2.3), and in 1987 it was refined by Eaton and Glickel to include scaphotrapezial joint

degeneration in the Stage IV criteria [12]. These classification systems are the most commonly used in clinical settings due to their objectivity and simplicity [14, 16]. The intra- and inter-observer reliabilities of the Eaton systems have been evaluated, and poor to moderate results were obtained [14, 16-20]. The view that is used to evaluate the joint has been shown to influence the outcome of the evaluation and agreement between evaluators. Dela Rose et al reported that mean kappa values for both intra- and inter-observer agreement were the highest when PA, lateral, and Bett's views were all used as opposed to using only one set of views [19].

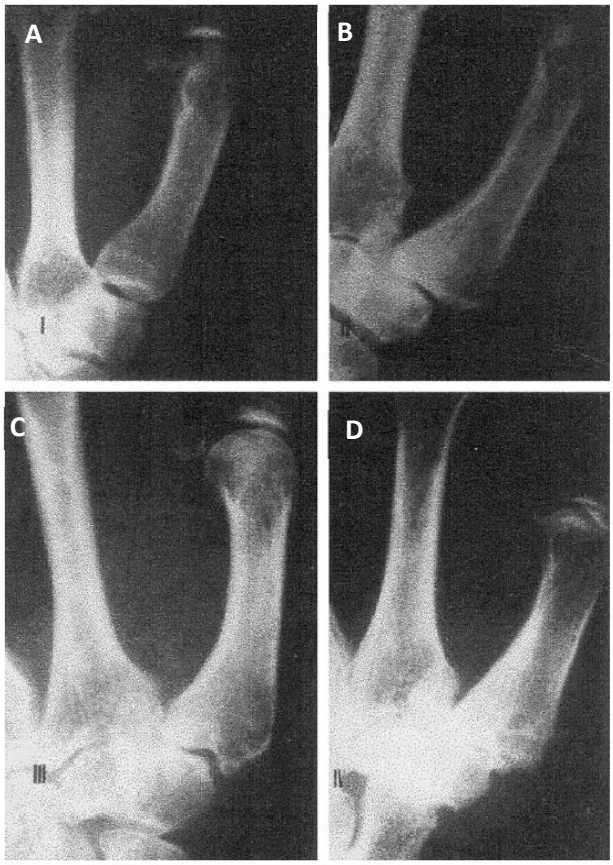

Figure 2.3 Definition of E-L radiographic OA stages: A – Stage I osteoarthritis B – Stage II osteoarthritis C – Stage III osteoarthritis D – Stage IV osteoarthritis (Used with permission from The Journal of Hand Surgery (American Ed.), 2002; 27: 882-885)

Arthroscopy is an operative tool that can be used to provide excellent visualization of the articular surfaces to determine the severity of OA within the joint [21, 22]. Two of the most

common classification systems used for arthroscopic evaluation are the Outerbridge and International Cartilage Repair Society (ICRS) [23]. Past clinical and cadaveric studies have reported poor agreement between radiographic and arthroscopic/visual assessments of the basilar thumb joint [24-26]. To our knowledge, there have not been any published studies attempting to draw correlations between arthroscopic OA grades and the amount of radiographic subluxation.

The role of subluxation in diagnosing OA in the basilar thumb joint has been under debate. Subluxation criteria was included in all four stages in Eaton and Littler's original classification system [4] but was only included in stage III when Eaton and Glickel revised it in 1987 [12]. While it has been thought to be an indicator of OA, some studies have speculated that subluxation in the joint can occur naturally in asymptomatic patients [27-29]. Other studies suggest that subluxation is different between men and women [30, 31], which would make it unreliable as a sole criterion for determining the OA stage. Further investigation into the relationship between radiographic subluxation and OA stage could reinforce its use as a diagnostic tool as well as contribute to the growing knowledge about the role of ligamentous laxity in OA progression.

The basilar thumb joint lacks substantial geometric constraint and therefore is reliant on ligaments and soft tissue for stability. Increased amounts of dorsoradial translation of the metacarpal have been reported with greater arthritic wear in the basilar thumb joint [5, 32]. The two ligaments that are believed to be the most important in preventing dorsoradial translation of the metacarpal with respect to the trapezium are the palmar anterior oblique ligament (AOL) and the dorsoradial ligament (DRL) [5, 32-34]. There is not a consensus on the contribution of each ligament to the overall stability of the joint. Initial cadaveric and biomechanical studies reported that the AOL was the primary stabilizer of the joint and prevented dorsal translation of the

metacarpal [5, 32, 35]. However, more recent studies have reported that the DRL plays a larger role in maintaining stability of the joint [33, 34, 36-39]. The joint capsule provides some structure for the joint and includes integration with stabilizing ligaments, but to our knowledge nobody has quantified the effect that disrupting the joint capsule has on the joint's stability.

This study had three objectives. The first objective was to determine which imaging angle would provide the best view of the full amount of lateral subluxation during simulated key pinch, the second objective was to compare the lateral subluxation of the metacarpal during key pinch with radiographic and visual OA grades, and the third objective was to determine the effect that opening the joint capsule and cutting the AOL had on the lateral subluxation of the metacarpal during key pinch. We hypothesized that the percent of subluxation would significantly correlate with the radiographic and arthroscopic/visual classifications and that sectioning the capsule and/or the AOL would significantly increase the amount of lateral subluxation.

2.3 Methods

Eleven frozen cadaveric forearms (10 males and 1 female, average age at death = 72 years, range 54-88 years at time of death) were obtained with no history of connective tissue disease. Anatomic dissection of each specimen was performed to isolate specific muscles necessary to simulate static key pinch. An initial incision was made down to the bone circumferentially in the proximal 1/3 of the forearm, followed by circumferential skin incision at the wrist; skin was then excised from the palmar and dorsal hand along the 4th metacarpal and across the metacarpal phalangeal joints to a point in the distal 1st web space. Skin was then removed along with palmar fascia in the hand and forearm to expose underlying tendons, transverse carpal ligament, and muscle. The mid-forearm was dissected to isolate tendons for the extensor pollicis longus (EPL), flexor pollicis longus (FPL), and abductor pollicis longus (APL).

The radius and ulna were then cleared of soft tissue, and care was taken to leave the transverse carpal ligament, interosseous membrane, and all wrist ligaments intact. The hand was meticulously dissected to isolate and elevate the origins of the abductor pollicis brevis (APB) along with the radial portion of the flexor pollicis brevis (FPB) as one group. The adductor pollicis (ADP) along with the ulnar portion of the FPB were isolated as another group [5]. Two holes were drilled in the radius and one in the ulna, anterior to posterior, to enable mounting of the forearm with plastic threaded rods to a radiolucent plastic plate in a neutral rotation. To simplify the experiments and provide consistent loading conditions, Kirschner wires were used to fix the wrist in 30º of extension, the thumb metacarpophalangeal (MP) joint was fixed in 20º of flexion, and the index finger MP joint was fixed at 90º. For three specimens intended for an additional study with MRI, carbon-fiber rods were used in place of Kirschner wires. Krackow suture loops using a 3-0 braided stitch were added to the end of each tendon or muscle group that would allow for application of static loads through a pulley system using water weights (Figure 2.4). The loads applied were borrowed from a previous experiment performed by Pellegrini et al. and were 0.8 N, 4.2 N, 5.0 N, 8.4 N, and 13.4 N for the EPL, ADP group, APB group, FPL, and APL, respectively [5]. Concurrent loading of all the tendons and groups was used to simulate static key pinch.

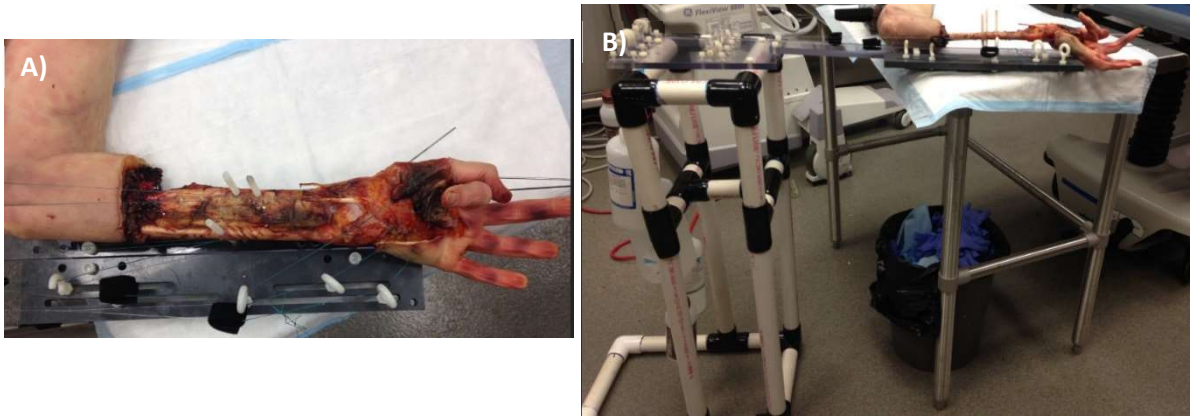

Figure 2.4 Water weights were applied to the EPL, ADP, APB, FPL, and APL to simulate key pinch. Adjustable eye bolts were used in slots to make adjustments for each specimen to maintain the muscles' anatomic line of action during weight application. A – Top view of the experimental setup B – Side view of the experimental setup

During load application, a mobile C-Arm unit (OrthoScan HD model 1000-0004) was used to acquire three sets of radiographs. Images were recorded from 0° (the hand AP view) with the top of the C-arm rotated by 5º increments towards the ulnar aspect of the arm up to 60º. This simulates supination of the hand in the AP view. This was done to determine which imaging angle best captured the full level of lateral subluxation for optimal evaluation of joint instability. The first set of images was taken with an intact joint capsule and anterior oblique ligament with weights applied to the previously specified tendons to simulate key pinch. This first set of images was used to determine the best angle to view lateral subluxation for subsequent analyses. Then the weights were removed and the joint capsule was opened between the AOL and the APL. The weights were applied and another set of images was recorded. Afterwards, the weights were removed again and the AOL was cut. The weights were reapplied and the final set of images was recorded. The total testing time for each specimen, from dissection to imaging, lasted approximately 2.5 hours. Specimen tissues were kept moist throughout testing with a saline solution.

Images were analyzed in Adobe Photoshop 6.0 to determine the percent lateral subluxation of the metacarpal base. The subluxation percentage was defined by the extent to which the metacarpal base extended past the trapezium divided by the total width of the metacarpal base (Figure 2.5). For each specimen, the maximum subluxation was used to normalize subluxations from the other image views to reduce the effect of inter-specimen variability. A frequency analysis of the maximum normalized subluxation was performed to determine which imaging angle best captured the maximum subluxation with an intact joint capsule. To further verify the best imaging angle, we evaluated percent differences (errors) in the normalized subluxation measurements for every angle in each specimen. These percent differences were then averaged across specimens for each imaging angle. The imaging angle that recorded the maximum subluxation most frequently and had smallest subluxation percent difference was then used for all further comparisons. The average absolute maximum subluxation from each imaging angle was compared to the average OA grades from their respective specimens. This was done to determine if there was a noticeable trend that would indicate if greater absolute subluxation was recorded as the imaging angle increased and if more severe OA was found in specimens that presented larger subluxation at increased imaging angles.

Figure 2.5 The method for measuring lateral subluxation using the boundary lines parallel to the metacarpal central axis. Subluxation percentage is calculated by dividing the lateral subluxation (DS) by the width of the metacarpal base or articular width (AW).

Radiographic and visual grading of the specimens was performed by an orthopedic resident using the Eaton-Littler scale for radiographic grades, and arthroscopic/visual grades were assigned using the Outerbridge and ICRS systems. Disarticulation of the joints for visual examination and classification of OA was performed after all of the necessary radiographic images were recorded. Subclassifications for the ICRS grading system, such as 1a and 1b grades, were grouped together for comparison to other grading systems and statistical analysis. Regression analysis of maximum absolute subluxation with radiographic and visual OA grades was performed to determine if there were any significant correlations. Statistical significance was set at $p < 0.05$. Repeated measures ANOVA with Brown-Forsythe post-hoc analysis was used to examine the significance of the relationship between the absolute subluxation measurements of the metacarpal for the intact joint capsule, the open joint capsule, and the transected AOL conditions. Statistical significance was set at $p < 0.05$. SAS was used for all statistical analyses.

2.4 Results

1. Subluxation View Determination

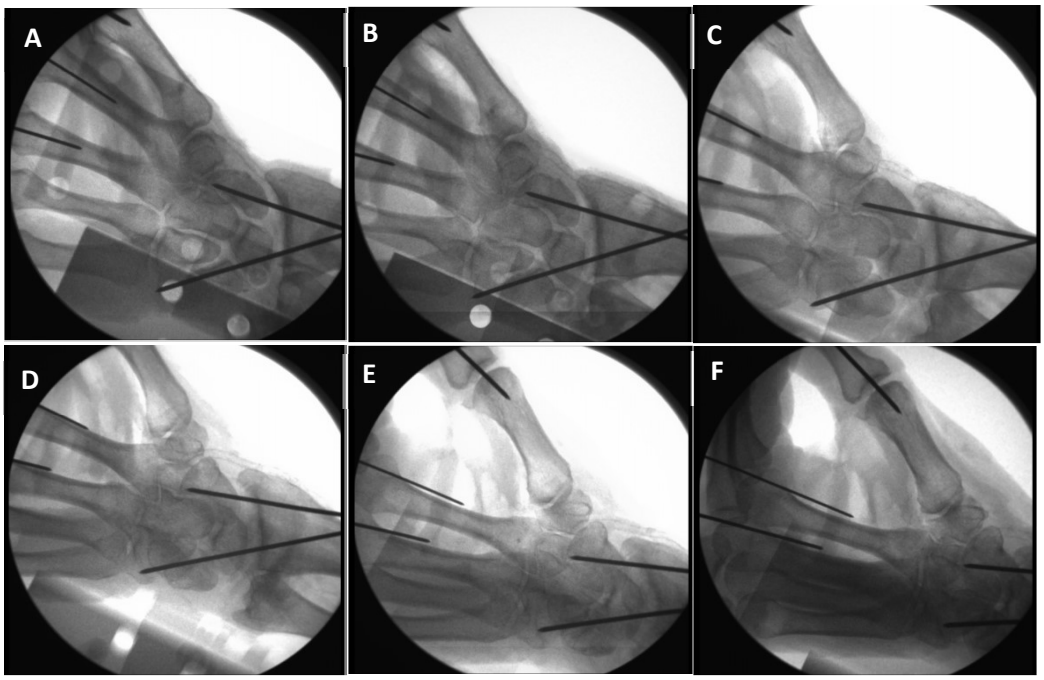

Figure 2.6 A – Radiographs of the same specimen at 0° (AP view) B – 10° C – 25° D – 35° E – 50° F - 60°. Only angles from 0° to 25° were analyzed for subluxation.

The lateral subluxation could not be consistently measured for image angles from 30º-60º due to the orientation of the joint and articular surfaces, so only data from 0º (AP view) to 25º were used for analysis of the imaging angle (Figure 2.6). The most common view that displayed the maximum subluxation was the AP view (0º) (Figure 2.7).

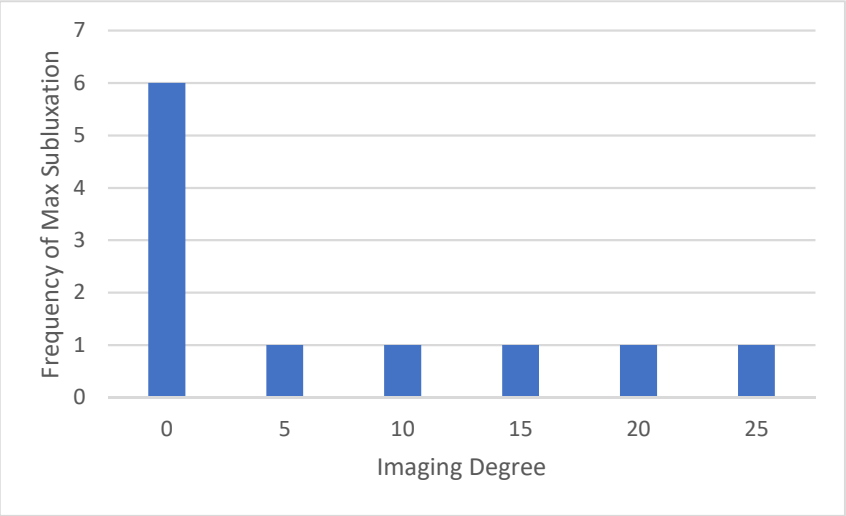

Figure 2.7 Number of specimens for which the maximum subluxation was measured at each imaging angle, with the joint capsule intact. Most of the specimens showed the maximum amount of subluxation when imaging was done at zero degrees (AP view).

The average percent difference from the measured maximum subluxation was the smallest in the AP view. Average maximum subluxation percent difference increased as the imaging angled increased (Figure 2.8).

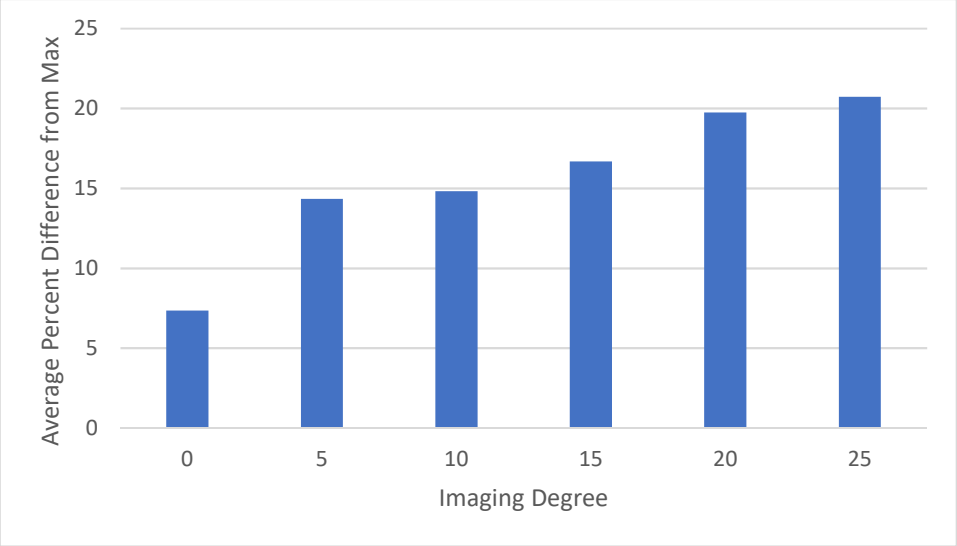

Figure 2.8 Average percent difference from a maximum normalized subluxation across specimens. Average percent difference was smallest for 0° (AP view) and increased with rotation angle.

The average absolute subluxation for each imaging angle was compared to the average OA grades from the specimens that showed maximum subluxation at that angle (Table 2.1). There were not any consistent trends for either absolute subluxation or OA grade as the imaging angle increased. However, it was noted that imaging angles of 20° and 25° were associated with the second highest and highest subluxations, and both had an Eaton-Littler grade of 4. The 25° imaging angle also had Outerbridge and ICRS grades of 4.

Table 2.1 Average Absolute Subluxation and OA Grades by Imaging Angle

Angle	0	5	10	15	20	25
Average Subluxation	31%	20%	22%	15%	43%	60%
Average Eaton-Littler Grade	2.166667	2	2	1	4	4
Average Outerbridge Grade	3	1	3	3	2	4
Average ICRS Grade	2.5	1	3	2	1	4

2. Subluxation and OA Classifications

According to the Outerbridge classification system seven of the eleven (64%) specimens had a grade of 3 or 4 which indicates a large amount of cartilage fragmentation or erosion of cartilage down to the bone. Three of the eleven (27%) had a grade of 2 which indicates some fragmentation of the articular cartilage, and one of the eleven (9%) had a grade of 1 which indicates cartilage with softening and swelling. According to the ICRS classification system six of the eleven (55%) had a grade which indicated significant defects or penetration to the subchondral bone, and the other five specimens (45%) had a grade which indicated either superficial fissures or lesions less than 50% of the cartilage depth in length. According to the Eaton-Littler radiographic classification system three of the eleven (27%) were stage I, three of the eleven (27%) were stage II, three of the eleven (27%) were stage III, and two of the eleven

(19%) were stage IV. There was not a significant correlation between absolute subluxation at 0º and the Outerbridge rating (p= 0.8018) nor with the ICRS rating (p= 0.7001). There was a significant correlation between percent subluxation and the Eaton-Littler radiographic rating (p= 0.0003, R^2 = 0.779).

3. Effect of opening Joint Capsule and Sectioning AOL

Absolute subluxation at a 0º imaging angle showed substantial variation for the intact joint capsule (mean = 31.7%, SD = 15.6%) (Figure 2.9). There were no statistical differences between the measured subluxations with the intact joint capsule, with the open joint capsule (mean = 35.3%, SD = 17.1%), nor with the sectioned/cut AOL (mean = 33.9%, SD = 17.2%) from repeated measure ANOVA (F[2, 20] = 1.32, p = 0.29).

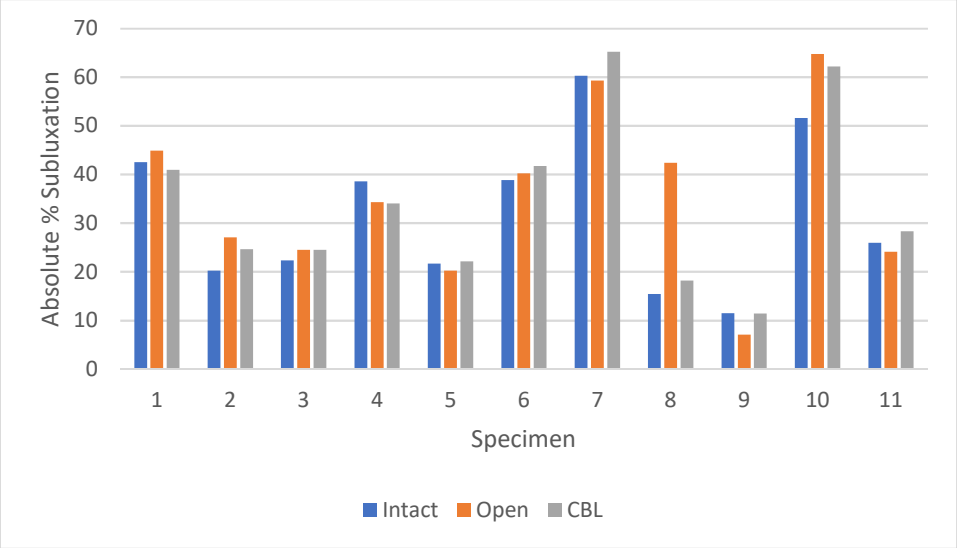

Figure 2.9 The percent subluxation for each specimen (for AP images only).

2.5 Discussion

The first objective of this study was to determine the best imaging angle for measuring subluxation during a key pinch stress radiograph. The presence of increased subluxation

measurements, and accompanying severity of OA in those specimens, may suggest that extreme OA may be better evaluated at 25°. However, this was only one specimen and several other specimens with grade 3 or 4 OA showed their highest subluxation at 0°, further reinforcing the choice of 0°. Some similar variation in the potential patient population is likely, but a consistent diagnostic tool for OA could still be useful for physicians in the clinic. Stress view radiographs provide insight that can help quantify the instability of the joint noted during physical examinations, and a few reported studies have focused on subluxation of the first metacarpal during key pinch [40, 41]. Cheema et al investigated the effects of open wedge trapezial osteotomy on contact location and metacarpal subluxation. They recorded radiographic images only from the AP view and reported that radial subluxation was significantly reduced after osteotomy was performed [41]. Adams et al investigated the effects of activation of the first dorsal interosseous (FDI) muscle and opponens pollicis (OP) to reduce subluxation of the first metacarpal and concluded that a muscle loading regime could exist that reduces subluxation [40]. However, Adams et al did not explicitly state which views they used to analyze lateral subluxation. Our study sought to verify the best view for subluxation analysis for future studies like these. The oblique orientation of the basilar thumb joint created some difficulties when attempting to analyze subluxation in the images due to its position and overlap between some of the bones. As the imaging angle increased the rotation caused overlap between the metacarpal base and radial edge of the trapezium which increased the difficulty in determining the amount of subluxation (Figure 6). The change in orientation also caused subluxation measurements to diverge from the maximum subluxation and increase the magnitude of the measurement error. Thus, our findings suggest that the AP view during key pinch provides the best assessment of

lateral subluxation. This finding should aid future efforts in the evaluation of subluxation within the basilar thumb joint.

The second objective of our study was to evaluate any correlations between the amount of lateral subluxation during key pinch and the visual and radiographic grades of OA. Our hypothesis was partially confirmed with a significant correlation between subluxation and the radiographic Eaton-Littler classification. Eaton and Littler defined broad criteria for subluxation in each stage of OA, so our significant correlation with their grading system is not surprising. We did not find a correlation between subluxation and either of the intraoperative (visual) classifications which provide more accurate assessments than radiographic analysis. Studies that have compared radiographic grades to patient symptom severity or visual inspections of the joint articular surfaces have not found good agreement between them [24-26]. Our results are consistent with these studies, as 45% of the specimens had severe arthritis (stage III or stage IV) from the Eaton-Littler classification compared to 64% and 55% from the Outerbridge and ICRS classifications, respectively. The lack of a significant correlation between subluxation and the more accurate visual grading systems may raise the question of its validity as a diagnostic tool, but some considerations must be kept in mind. The Outerbridge and ICRS classification systems do not include subluxation in their staging criteria. The differences in magnitude of our absolute subluxation measurements are influenced by inter-specimen variability, and these values are being compared to visual classification systems that, while considered more accurate, are naturally defined by generalized staging criteria. Thus, it might be difficult to correlate highly individualized data to any generalized rating system. Further studies into the relationship between subluxation and the visual and symptomatic severity of OA are warranted to continue to shape the diagnostic role of metacarpal subluxation.

A limited number of studies have looked for possible correlations between the amount of metacarpal subluxation and patient symptoms or radiographic OA grades. Riordan et al examined the relationship between radiographic OA grade and subluxation measured during the stress test described by Wolf et al [6], and they found that lower subluxation percentages were present in patients with more advanced disease [42]. This is in contrast to our findings of increased subluxation with increasing severity of radiographic OA. It must be noted that there are critical differences when comparing the results of the two studies. Our study utilized key pinch instead of Wolf's modifications to the Eaton-Littler stress radiograph to measure subluxation. This may have affected the amount of activity by each of the supporting ligaments. Wolfe et al noted that their method is likely to recruit all of the primary ligamentous stabilizers while key pinch may not. The metacarpal may be located in slightly different positions between abduction and adduction and therefore stability may be more affected by either the AOL or the DRL [43, 44]. Another key difference between the two studies is that Riordan et al performed a clinical study while ours was a cadaveric study. Though Riordan et al. advise caution about drawing correlations between greater subluxation and increased OA stage, our results support previous assertions that subluxation can be used as an indicator of OA in the basilar thumb joint and may be used to supplement radiographic grading. While radiographic grading is not as accurate as grading after visual examination, it provides a less-invasive method to examine the joint and our results support stress view radiographs can additionally be used to confirm the joint's instability and severity of OA.

In addition to investigating if subluxation could be used as an indicator for OA, the final objective in this study was to examine the effects of opening the joint capsule between the AOL and the APL and sectioning the AOL on lateral subluxation of the 1st metacarpal. The AOL is a

capsular ligament, so to be able to evaluate the capsule separately it was opened first. The fact that we found no significant difference in maximum subluxation with sectioning the capsule or AOL appears to support more recent studies indicating that the AOL plays a lesser role in the prevention of dorsal subluxation of the metacarpal [33, 36-38]. However, the old age of our specimens at the time of death and advanced arthritic states could have influenced the subluxation results. For instance, Pellegrini et al. noted that specimens with more advanced arthritis experienced less dorsal subluxation and contact pattern change after transection of the AOL [5]. A few similar studies have sought to characterize the translation of the first metacarpal during key pinch after sectioning of different ligaments, and they have reported conflicting results [5, 33, 45]. Pellegrini et al noted contact was primarily on the palmar portion of the joint with dorsal translation of the metacarpal after sectioning the AOL [5]. Colman et al reported that transection of the AOL during key pinch resulted in increased ulnar and palmar translation whereas transection of the DRL resulted in increased radial and palmar translation [33]. Esplugas et al reported that transection of dorsal ligaments resulted in substantially larger dorsoradial translation than either volar or ulnar ligaments [45]. While studies have differed on the relative importance of the DRL and AOL, it is likely that both have important contributions to the joint's stability. Care must be taken not to interpret the results of this study as direct evidence for the role of the DRL or other supporting ligaments in preventing dorsal subluxation.

The lack of significant change in the amount of subluxation after transection of the AOL also entertains the suggestion that a critical source for stability of the joint could come from dynamic muscular activity, but this hypothesis would be difficult to test in cadaveric studies. Computational models that analyze the recruitment patterns of different ligaments during functional activities and anatomical motions could supplement cadaveric biomechanical studies.

A few such studies have already been reported with some contradictory results [43, 44, 46]. Further cadaveric studies, in addition to computational studies investigating the recruitment patterns of the AOL and DRL, will help to define each ligament's function within the thumb's range of motion.

This study has several limitations. Both visual and radiographic OA grades were assigned by only one investigator. However, inter-rater reliability for radiographic analysis of the basilar thumb joint has been established as poor to moderate [14, 16-20]. An increased number of investigators grading the joints could produce averaged OA grades that have an adverse effect on the significance of the relationships examined in our comparisons. Subluxation was measured by only one of the investigators, and the subluxation measurement is subject to small potential errors estimating on the bone boundaries on the digital images. However, we estimate these small errors would be on the order of 2-4% of the subluxation measurement. Most cadaveric specimens were quite old and were kept in frozen storage before the experiments. This could have affected the material properties of all the soft tissues and their response during simulated key pinch. Only one cadaveric specimen was female so no analysis of gender differences was possible. Subluxation for the female specimen was within the variance of the male specimens.

In conclusion, we tested eleven cadaveric specimens in simulated key pinch and recorded radiographic images over a select range of imaging angles. We found that the AP view provided the best visualization of lateral subluxation of the metacarpal. Key pinch is already used in the diagnostic process for basilar thumb joint OA, and AP images taken during a daily task such as key pinch will require little instruction and decrease the possible confusion for patients during examinations while quantifying the instability of the joint. The Outerbridge and ICRS visual grading systems of the joint did not significantly correlate with the amount of subluxation in the

joint, but the Eaton-Littler radiographic grade expectedly correlated with subluxation. This finding supports the assertion that subluxation can be used as an indicator of OA while using the Eaton-Littler radiographic grading system. The significant correlation to radiographic grades underscores that a key pinch stress radiograph could be used as a tool by physicians to quantitatively assess joint instability. The joint capsule was opened and the AOL was cut to determine their effects on lateral subluxation, and we found that neither had a significant effect. This supports recent research that the AOL may not play a large role in the basilar thumb joint's stability during key pinch [33, 43, 46].

2.6 References

1. Dahaghin, S., S.M. Bierma-Zeinstra, A.Z. Ginai, H.A. Pols, J.M. Hazes, and B.W. Koes, *Prevalence and pattern of radiographic hand osteoarthritis and association with pain and disability (the Rotterdam study).* Ann Rheum Dis, 2005. **64**(5): p. 682-7.
2. Wilder, F.V., J.P. Barrett, and E.J. Farina, *Joint-specific prevalence of osteoarthritis of the hand.* Osteoarthritis Cartilage, 2006. **14**(9): p. 953-7.
3. Billing, L. and K.-O. Gedda, *Roentgen examination of Bennett's fracture.* Acta radiologica, 1952(6): p. 471-476.
4. Eaton, R.G. and J.W. Littler, *Ligament reconstruction for the painful thumb carpometacarpal joint.* J Bone Joint Surg Am, 1973. **55**(8): p. 1655-66.
5. Pellegrini, V.D., Jr., C.W. Olcott, and G. Hollenberg, *Contact patterns in the trapeziometacarpal joint: the role of the palmar beak ligament.* J Hand Surg Am, 1993. **18**(2): p. 238-44.

6. Wolf, J.M., T.W. Oren, B. Ferguson, A. Williams, and B. Petersen, *The carpometacarpal stress view radiograph in the evaluation of trapeziometacarpal joint laxity.* J Hand Surg Am, 2009. **34**(8): p. 1402-6.

7. Wolf, J.M., S. Schreier, S. Tomsick, A. Williams, and B. Petersen, *Radiographic laxity of the trapeziometacarpal joint is correlated with generalized joint hypermobility.* J Hand Surg Am, 2011. **36**(7): p. 1165-9.

8. Barron, O.A. and R.G. Eaton, *Save the trapezium: double interposition arthroplasty for the treatment of stage IV disease of the basal joint.* J Hand Surg Am, 1998. **23**(2): p. 196-204.

9. McQuillan, T.J., D. Kenney, J.J. Crisco, A.P. Weiss, and A.L. Ladd, *Weaker Functional Pinch Strength Is Associated With Early Thumb Carpometacarpal Osteoarthritis.* Clin Orthop Relat Res, 2016. **474**(2): p. 557-61.

10. Villafane, J.H., K. Valdes, L. Bertozzi, and S. Negrini, *Minimal Clinically Important Difference of Grip and Pinch Strength in Women With Thumb Carpometacarpal Osteoarthritis When Compared to Healthy Subjects.* Rehabil Nurs, 2017. **42**(3): p. 139-145.

11. Halilaj, E., D.C. Moore, T.K. Patel, A.L. Ladd, A.P. Weiss, and J.J. Crisco, *Early osteoarthritis of the trapeziometacarpal joint is not associated with joint instability during typical isometric loading.* J Orthop Res, 2015. **33**(11): p. 1639-45.

12. Eaton, R.G. and S.Z. Glickel, *Trapeziometacarpal osteoarthritis. Staging as a rationale for treatment.* Hand Clin, 1987. **3**(4): p. 455-71.

13. Kurosawa, K., I. Tsuchiya, and K. Takagishi, *Trapezial-metacarpal joint arthritis: radiographic correlation between first metacarpal articular tilt and dorsal subluxation.* J Hand Surg Am, 2013. **38**(2): p. 302-8.

14. Spaans, A.J., C.M. van Laarhoven, A.H. Schuurman, and L.P. van Minnen, *Interobserver agreement of the Eaton-Littler classification system and treatment strategy of thumb carpometacarpal joint osteoarthritis.* J Hand Surg Am, 2011. **36**(9): p. 1467-70.

15. Bettinger, P.C., R.L. Linscheid, W.P. Cooney, 3rd, and K.N. An, *Trapezial tilt: a radiographic correlation with advanced trapeziometacarpal joint arthritis.* J Hand Surg Am, 2001. **26**(4): p. 692-7.

16. Choa, R.M. and H.P. Giele, *Inter- and intrarater reliability of osteoarthritis classification at the trapeziometacarpal joint.* J Hand Surg Am, 2015. **40**(1): p. 23-6.

17. Becker, S.J., W.E. Bruinsma, T.G. Guitton, C.M. van der Horst, S.D. Strackee, and D. Ring, *Interobserver Agreement of the Eaton-Glickel Classification for Trapeziometacarpal and Scaphotrapezial Arthrosis.* J Hand Surg Am, 2016. **41**(4): p. 532-540.e1.

18. Kubik, N.J., 3rd and J.D. Lubahn, *Intrarater and interrater reliability of the Eaton classification of basal joint arthritis.* J Hand Surg Am, 2002. **27**(5): p. 882-5.

19. Dela Rosa, T.L., M.C. Vance, and P.J. Stern, *Radiographic optimization of the Eaton classification.* J Hand Surg Br, 2004. **29**(2): p. 173-7.

20. Hansen, T.B., O.G. Sorensen, L. Kirkeby, M. Homilius, and A.L. Amstrup, *Computed tomography improves intra-observer reliability, but not the inter-observer reliability of the Eaton-Glickel classification.* J Hand Surg Eur Vol, 2013. **38**(2): p. 187-91.

21. Badia, A., *Arthroscopy of the trapeziometacarpal and metacarpophalangeal joints.* J Hand Surg Am, 2007. **32**(5): p. 707-24.

22. Berger, R.A., *A technique for arthroscopic evaluation of the first carpometacarpal joint.* J Hand Surg Am, 1997. **22**(6): p. 1077-80.

23. Spahn, G., H.M. Klinger, and G.O. Hofmann, *How valid is the arthroscopic diagnosis of cartilage lesions? Results of an opinion survey among highly experienced arthroscopic surgeons.* Arch Orthop Trauma Surg, 2009. **129**(8): p. 1117-21.

24. Brown, G.D., 3rd, M.S. Roh, R.J. Strauch, M.P. Rosenwasser, G.A. Ateshian, and V.C. Mow, *Radiography and visual pathology of the osteoarthritic scaphotrapezio-trapezoidal joint, and its relationship to trapeziometacarpal osteoarthritis.* J Hand Surg Am, 2003. **28**(5): p. 739-43.

25. Glickel, S.Z., A.N. Kornstein, and R.G. Eaton, *Long-term follow-up of trapeziometacarpal arthroplasty with coexisting scaphotrapezial disease.* J Hand Surg Am, 1992. **17**(4): p. 612-20.

26. North, E.R. and R.G. Eaton, *Degenerative joint disease of the trapezium: a comparative radiographic and anatomic study.* J Hand Surg Am, 1983. **8**(2): p. 160-6.

27. Dumont, C., S. Lerzer, M.A. Vafa, M. Tezval, P. Dechent, K.M. Sturmer, and J. Lotz, *Osteoarthritis of the carpometacarpal joint of the thumb: a new MR imaging technique for the standardized detection of relevant ligamental lesions.* Skeletal Radiol, 2014. **43**(10): p. 1411-20.

28. Larsen, S.K., A.M. Ostergaard, and T.B. Hansen, *The influence of subluxation on the severity of symptoms, disability, and the results of operative treatment in TMC osteoarthritis with total joint arthroplasty.* Hand (N Y), 2015. **10**(4): p. 593-7.

29. Rust, P.A., E.T.H. Ek, and S.K.Y. Tham, *Assessment of normal trapeziometacarpal joint alignment.* J Hand Surg Eur Vol, 2017. **42**(6): p. 605-609.

30. de Raedt, S., M. Stilling, M. van de Giessen, G.J. Streekstra, F.M. Vos, and T.B. Hansen, *A three-dimensional analysis of osteoarthritic changes in the thumb carpometacarpal joint.* J Hand Surg Eur Vol, 2013. **38**(8): p. 851-9.

31. Halilaj, E., M.J. Rainbow, C. Got, J.B. Schwartz, D.C. Moore, A.P. Weiss, A.L. Ladd, and J.J. Crisco, *In vivo kinematics of the thumb carpometacarpal joint during three isometric functional tasks.* Clin Orthop Relat Res, 2014. **472**(4): p. 1114-22.

32. Doerschuk, S.H., D.G. Hicks, V.M. Chinchilli, and V.D. Pellegrini, Jr., *Histopathology of the palmar beak ligament in trapeziometacarpal osteoarthritis.* J Hand Surg Am, 1999. **24**(3): p. 496-504.

33. Colman, M., D.P. Mass, and L.F. Draganich, *Effects of the deep anterior oblique and dorsoradial ligaments on trapeziometacarpal joint stability.* J Hand Surg Am, 2007. **32**(3): p. 310-7.

34. Van Brenk, B., R.R. Richards, M.B. Mackay, and E.L. Boynton, *A biomechanical assessment of ligaments preventing dorsoradial subluxation of the trapeziometacarpal joint.* J Hand Surg Am, 1998. **23**(4): p. 607-11.

35. Imaeda, T., G. Niebur, K.N. An, and W.P. Cooney, 3rd, *Kinematics of the trapeziometacarpal joint after sectioning of ligaments.* J Orthop Res, 1994. **12**(2): p. 205-10.

36. Bettinger, P.C., W.P. Smutz, R.L. Linscheid, W.P. Cooney, 3rd, and K.N. An, *Material properties of the trapezial and trapeziometacarpal ligaments.* J Hand Surg Am, 2000. **25**(6): p. 1085-95.

37. D'Agostino, P., F.D. Kerkhof, M. Shahabpour, J.P. Moermans, F. Stockmans, and E.E. Vereecke, *Comparison of the anatomical dimensions and mechanical properties of the dorsoradial and anterior oblique ligaments of the trapeziometacarpal joint.* J Hand Surg Am, 2014. **39**(6): p. 1098-107.

38. Ladd, A.L., J. Lee, and E. Hagert, *Macroscopic and microscopic analysis of the thumb carpometacarpal ligaments: a cadaveric study of ligament anatomy and histology.* J Bone Joint Surg Am, 2012. **94**(16): p. 1468-77.

39. Strauch, R.J., M.J. Behrman, and M.P. Rosenwasser, *Acute dislocation of the carpometacarpal joint of the thumb: an anatomic and cadaver study.* J Hand Surg Am, 1994. **19**(1): p. 93-8.

40. Adams, J.E., V. O'Brien, E. Magnusson, B. Rosenstein, and D.J. Nuckley, *Radiographic Analysis of Simulated First Dorsal Interosseous and Opponens Pollicis Loading Upon Thumb CMC Joint Subluxation: A Cadaver Study.* Hand (N Y), 2018. **13**(1): p. 40-44.

41. Cheema, T., C. Salas, N. Morrell, L. Lansing, M.M. Reda Taha, and D. Mercer, *Opening wedge trapezial osteotomy as possible treatment for early trapeziometacarpal osteoarthritis: a biomechanical investigation of radial subluxation, contact area, and contact pressure.* J Hand Surg Am, 2012. **37**(4): p. 699-705.

42. Riordan, E., S. Robbins, L. Deveza, V. Duong, W.M. Oo, A. Wajon, K. Bennell, J. Eyles, R. Jongs, J. Linklater, and D. Hunter, *Radial subluxation in relation to hand strength and radiographic severity in trapeziometacarpal osteoarthritis.* Osteoarthritis Cartilage, 2018.

43. Halilaj, E., M.J. Rainbow, D.C. Moore, D.H. Laidlaw, A.P. Weiss, A.L. Ladd, and J.J. Crisco, *In vivo recruitment patterns in the anterior oblique and dorsoradial ligaments of the first carpometacarpal joint.* J Biomech, 2015. **48**(10): p. 1893-8.

44. Imaeda, T., G. Niebur, W.P. Cooney, R.L. Linscheid, and K.-N. An, *Ligament length during circumduction of the trapeziometacarpal joint.* Journal of orthopaedic science, 1997. **2**(5): p. 319-327.

45. Esplugas, M., A. Lluch-Bergada, N. Mobargha, M. Llusa-Perez, E. Hagert, and M. Garcia-Elias, *Trapeziometacarpal Ligaments Biomechanical Study: Implications in Arthroscopy.* J Wrist Surg, 2016. **5**(4): p. 277-283.

46. Tan, J., J. Xu, R.G. Xie, A.D. Deng, and J.B. Tang, *In vivo length and changes of ligaments stabilizing the thumb carpometacarpal joint.* J Hand Surg Am, 2011. **36**(3): p. 420-7.

Chapter 3. Validation Criteria and Results for MRI-Based Modeling of Basilar Thumb Joint Contact Mechanics

3.1 Abstract

Different theories have been proposed as to how osteoarthritis (OA) develops in the basilar thumb joint. Past studies have used different techniques to experimentally measure contact area within the joint, but insertion of films or gels into the joint space and disruption of the joint capsule could affect contact location and measurements. Three-dimensional modeling techniques, such as image-based finite element modeling (FEM), can be used to measure in vivo contact pressures and locations without disrupting the joint capsule and other supportive soft tissues. To assure that finite element models provide accurate and useful approximations for research or clinical applications, they must be validated through comparisons with experimental data. Three upper extremity specimens were dissected and mounted to enable an experimental simulation of key pinch and measurement of different contact measures. Each specimen was also placed in a MRI machine to collect images in both an unloaded and simulated pinch condition for determination basilar thumb joint contact mechanics using FEM. FEM data was directly compared to experimental contact pressure data. Qualitative comparisons of the model and experimental contact patterns matched well for two of the three specimens. Contact force was the only contact measure that met validation criterion, and it was validated in all three specimens. Experimental contact areas were consistently larger than model results. The resolution of the Tekscan sensor, the stiffness of the material used to prevent contamination of the sensors, and the small size of the joint likely impacted the experimental measurements. These experimental difficulties supports the need for better experimental techniques as well as highlight the usefulness of computational modeling for the basilar thumb joint.

3.2 Introduction

The basilar thumb joint, also known as the trapeziometacarpal (TMC) or thumb carpometacarpal (CMC) joint, has the second highest incidence of OA in the hand [1]. OA in the basilar thumb joint is a debilitating disease that more commonly affects women than men [1, 2]. In addition, approximately 33% of postmenopausal women are affected by OA in this joint [3]. The development of OA is believed to be caused by both intrinsic factors, such as age and gender, and local factors, such as joint deformity, trauma, and excessive loading. Trauma to a joint or natural changes that gradually occur have been thought to shift contact to areas of articular cartilage that are not accustomed to joint loads, and this shift could incite OA and/or contribute to its progression [4, 5]. Several theories of abnormal joint loading have emerged to explain how abnormal joint mechanics contribute to the development of OA. The ligament laxity theory states that increasing laxity of critical stabilizing ligaments, such as the anterior oblique ligament (AOL) or the dorsoradial ligament (DRL), leads to dorsal translation of the metacarpal. This shifts contact to areas in the joint that are not accustomed to bearing loads as well as placing shear loads on the articular cartilage which increases degradation [6-10]. Another theory is that rotation of the metacarpal during tasks such as pinch and grip, along with incongruent joint surfaces, concentrates pressure on cartilage in the dorsoradial and volar-ulnar compartments of the joint that do not routinely bear joint loads which leads to degenerative changes [11-13]. Further understanding of contact mechanics and contact area locations in the basilar thumb joint would be useful for determining the validity of these theories, improving our knowledge of OA development and progression, developing methods to prevent OA in those at risk, and drive future innovative patient-specific treatments.

Past studies have sought to understand contact mechanics and patterns of the basilar thumb joint in cadaveric experiments using different methods such as silicone rubber casting [14], stereophotogrammetry [15], and pressure-sensitive Fuji films [8]. However, cadaveric studies cannot capture all the complexities of in vivo conditions such as support provided by soft tissues and dynamic stabilization from surrounding musculature. Computational modeling with geometries created from MR images [16, 17] or CT scans [18] provide a non-invasive option to study joint contact patterns and mechanics during active functional tasks. Common computational modeling techniques include finite element analysis (FEA) [19, 20], rigid body spring modeling (RBSM) [18, 21], and multi-body/surface contact modeling (SCM) [16, 17]. Methods such as SCM are computationally less expensive than FEA, but FEA is considered the most accurate method for calculating contact stresses [22, 23]. Outputs such as contact forces, areas, and pressure distributions can also be calculated using FEA. For any such technique to be considered reliable it must be first be validated against relevant experimental data. Indirect validation through comparison of specimen data to literature values is one option for validation, but direct validation through comparison of specimen data to specimen-specific models is the preferred approach [23].

The first objective of our study was to perform a direct validation of a MRI-based finite element modeling technique of the basilar thumb joint during simulated key pinch. This was done by comparison of experimental data obtained using a trimmed K-Scan^{TM} Wrist Sensor #4201 (Tekscan Inc., South Boston, MA, USA) and specimen-specific finite element model data obtained using MR images. The set validation criterion was that model data should/must fall within two times the standard deviation of the experimental measure [24]. The protocols used for this validation study were the same as for planned protocols for evaluating basilar thumb joint

mechanics in vivo. One common limitation of cadaveric studies is the disruption of soft tissue structures and the effect that disruption may have on the accuracy of experimental data. Thus, our second objective was to analyze the impact that opening the joint capsule would have on the contact mechanics. We hypothesized that opening the joint capsule would significantly change the average pressure (AP), peak pressure (PP), contact area (CA), and contact force (CF).

3.3 Methods

Three frozen cadaveric specimens were obtained that did not have a history of connective tissue disease (all male, age at death = 66, 76, and 83 years). Each specimen was anatomically dissected to isolate specific muscles and tendons that are necessary to perform static key pinch. The mid-forearm was dissected to isolate the flexor pollicis longus (FPL), abductor pollicis longus (APL), and the extensor pollicis longus (EPL). The radius and ulna were then cleared of the remaining soft tissue, and care was taken to leave the transverse carpal ligament, interosseous membrane, and volar wrist ligaments intact. The hand was dissected to isolate the radial portion of the flexor pollicis brevis (FPB) and the origin of the abductor pollicis brevis (APB) as one muscle group for weight application. The ulnar portion of the FPB along with the adductor pollicis (ADP) were used as another group for application weights for simulation of muscle forces [8]. All the materials used in the experimental setup were made of plastic, with water used for the weights, so that everything would be compatible with the MRI scanner. Two anterior to posterior holes were drilled in the radius and one in the ulna to allow for mounting with plastic threaded rods to a plastic plate in a neutral rotation. The wrist was fixed in 30° of the extension, the thumb metacarpophalangeal (MP) joint was fixed in 20° of flexion, and the index finger MP joint was fixed at 90° to provide consistent loading conditions. Krackow suture loops using a 3-0 braided stitch were attached to the end of each tendon or muscle group to allow for the

application of static loads with the water weights through a pulley system that approximated anatomical directions (Figure 3.1). Applied loads for the FPL, APL, EPL, APB group, and ADP group followed the methods of Pellegrini et al. and were 8.4 N, 13.4 N, 0.8 N, 5.0 N, and 4.2 N, respectively [8]. Concurrent loading of the all the tendons and groups was utilized to simulate static key pinch while collecting experimental pressure measurements and during the MRI scanning for FE modeling.

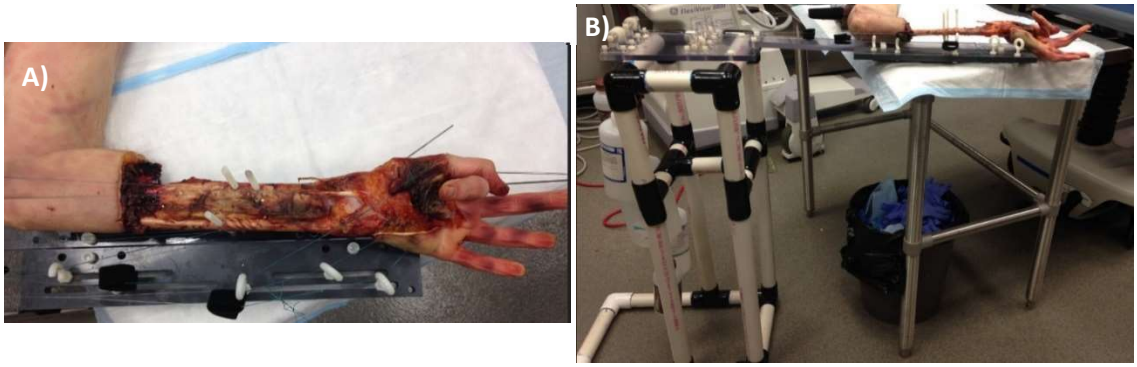

Figure 3.1 A – Top view of the experimental setup B – Side view of the experimental setup. Looped stitches were run through plastic eyebolts to maintain anatomical directions during loading and attached to their respective water weights. Slots were created for the eyebolts to allow for necessary placement adjustments for individual specimens to maintain proper anatomical lines of action for each muscle.

After dissection and setup and before experimental measurements were recorded, MR images were acquired for the specimens. MRI scans were performed using a dual echo steady state (DESS) sequence. Two types of image sets, “relaxed” and “pinch”, were acquired for each specimen. The relaxed image set was recorded when no external weights were applied to the specimen. The protocols were DESS during relaxed/unloaded scans with matrix: 448 x 240 pixels, FOV: 100 mm x 48 mm, slice thickness: 0.5 mm, scan time: 4.5 minutes. For loaded key pinch scans, the protocols were DESS with matrix: 320 x 320 pixels, FOV: 100 mm x 100 mm, slice thickness: 1.0 mm, scan time: 188 seconds**.** The first pinch image set was recorded when all

five of the external weights were applied and the joint capsule remained intact. The second pinch image set was recorded with the same loading conditions after an incision had been made in the joint capsule from the APL to the AOL for later insertion of the Tekscan sensor.

After MRI scanning, pressure measurements with an electronic pressure sensor were made in the basilar thumb joint during simulated key pinch. An electronic sensor designed for the wrist (Tekscan Inc., South Boston, MA, USA, Model #4201) was carefully trimmed into a 6x6 array of sensels to fit into the basilar thumb joint and provide maximum coverage of the joint surface area. It was resealed with packaging tape to avoid liquid contamination of the sensor. Equilibration and calibration of the sensors were performed before each experiment using Tekscan's standard instrumentation and procedures. Equilibration was performed to reduce variation between the pressure values registered by sensels when placed under a uniform load. Two-point power calibration of the sensors was performed using a Tekscan PB100E equilibration and calibration device. Pressures of 50 psi (0.34 MPa) and 75 psi (0.52 MPa) were used for the two-point calibration. During calibration the sensitivity of the sensors was increased to account for the increased stiffness from the packaging tape. The sensor was consistently oriented before insertion to allow for consistent analysis of the data across specimens. One set of data was collected for each specimen. Each data set consisted of 10 frames of contact data and was collected at a rate of 2 frames/second. Pressure was recorded by Tekscan as a numerical array and was visually displayed in a colored array of discrete sensels. The numerical array was manipulated and used for quantitative comparisons, and the color array was used for qualitative comparisons with model data. Average pressure, peak pressure, contact force, and contact area were recorded in each data frame. Radiographic and visual grading of the specimens was performed by an orthopedic resident using the Eaton-Littler scale for radiographic grades, and

arthroscopic/visual grades were assigned using the Outerbridge and ICRS systems. Disarticulation of the joints for visual examination and classification of OA was performed after all of the necessary MR images were recorded and experimental data was collected. The total testing time for each specimen, from dissection to imaging and experimental data collection, lasted four hours. Specimen tissues were kept moist throughout testing with a saline solution.

Manual segmentation of the MR images was performed using the software ScanIP. For the relaxed image set, the metacarpal, trapezium, and their respective cartilage surfaces were segmented to create three-dimensional models. For the pinch image sets, only the metacarpal and trapezium bones were segmented to use for the kinematic registration process. Kinematics for the models were determined through image registration using a combination of the software Analyze 5.0 (AnalyzeDirect, Overland Park, KS) and PreView to adjust registrations in 3D. The segmented bones for each image set were isolated on a black background to create new image stacks used in Analyze (Figure 3.2). The metacarpal was chosen as the reference bone and was used to align the coordinate systems of the image sets through registration of the loaded metacarpal to the unloaded metacarpal. Three-dimensional voxel matching of normalized mutual image intensity was used to maximize the 3D correspondence of the image sets and ignore areas the image sets did not share. Analyze provided a kinematic transformation of the alignment between the loaded metacarpal and the unloaded metacarpal, but it only shows orthogonal 2D views. PreView was used to check and help manually correct (as needed) the alignment in 3D. The trapezium from the pinch image set was then transformed to the unloaded image coordinate system using the transformation of the pinch metacarpal to the unloaded metacarpal. The last step for the kinematic determination was to register the trapezium from the relaxed image set to the transformed pinch trapezium image set. This step provided the final kinematic data that

would be applied in the modeling software as translation vectors and attitude vectors for rotation of the trapezium from a relaxed configuration to a pinch configuration. This transformation was placed on the trapezium geometry created from the relaxed image set to simulate its position and orientation during key pinch.

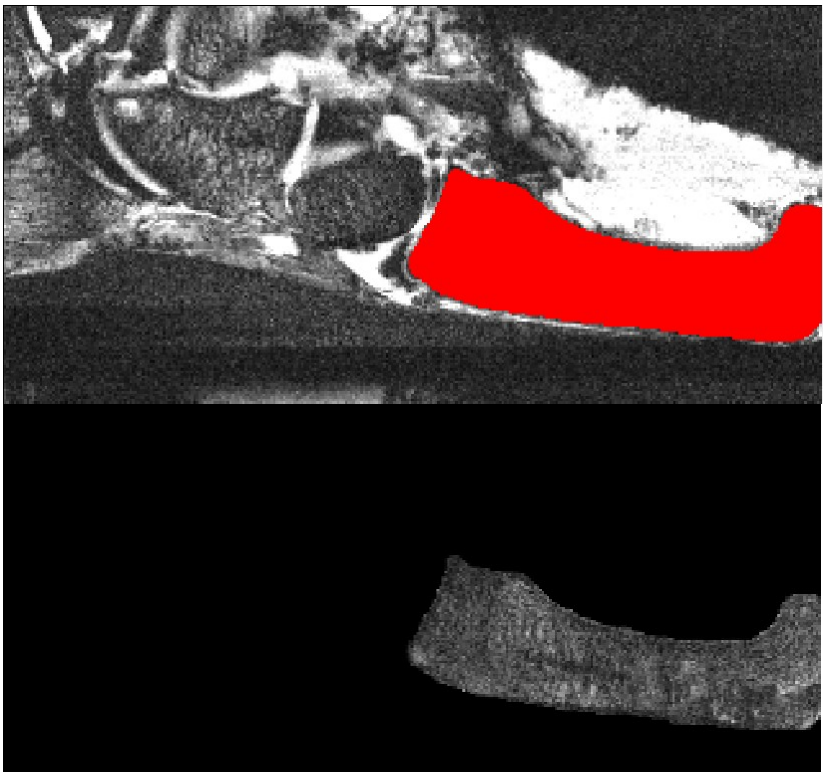

Figure 3.2 The process to create an image set for kinematic registration. Top image – Segmentation of the first metacarpal for the unloaded image set. Bottom image – Isolation of the first metacarpal on a black background.

The three-dimensional models of the bones and cartilage were meshed with linear tetrahedral elements. The meshes for the metacarpal and trapezium cartilage were refined to have a target element edge length of 0.40 mm. The meshed models were imported into PreView to apply the modeling boundary conditions. The fully defined models were then solved with FEBio [25] to analyze the contact mechanics. Cartilage was modeled as a neo-hookean, homogeneous, and isotropic deformable material. The instantaneous characteristics of articular cartilage are that of an incompressible material, but over time its compressibility increases with fluid efflux and

matrix compression. Thus, a Poisson's ratio $\nu = 0.20$ was used to model the long-term response of cartilage [26]. Due to the increased age of the specimens at their time of death, it was assumed that all the joints had been affected by osteoarthritis to some extent. Therefore, the Young's Modulus was assumed to be $E = 1.75$ MPa [27]. Bone was assumed to undergo negligible deformation during key pinch, thus it was modeled as a neo-hookean, homogeneous, and isotropic material with a Poisson's ratio $\nu = 0.30$ and a Young's Modulus $E = 12000$ MPa. Boundary conditions were placed on the distal end of the metacarpal to fix translation and rotation in all directions. Boundary conditions on the proximal end of the trapezium fixed rotation in all directions, fixed translation in the x- and z-directions, and prescribed translation in the y-axis to create a displacement-controlled model. Translation and rotation vectors taken from the final kinematic registration were used to place the trapezium in the loaded position. The contact between the articular surfaces was defined to be frictionless sliding contact. The model was then solved using FEBio version 2.5.2. The results were visualized and assessed using PostView. The average of the top 1% of 3rd principal stress values on the metacarpal articular surface was used for the model peak pressure. Average pressure was defined as the average of 3rd principal stress values on the metacarpal articular surface.

Custom code was written in Matlab to recalculate the contact force, contact area, average pressure, and peak pressure from the experimental data after applying a subtraction filter of 0.075 MPa (average pressure values) to remove residual pressure data recorded by the sensor. The Matlab code also removed the first data frame of each experimental data set before the calculations to remove any bias caused by the initial impact during joint loading. Afterwards, each parameter was recalculated in each frame and averaged over the nine remaining frames for comparisons to the model data. Contact force, contact area, average contact pressure, and peak

pressure collected using the Tekscan sensors were compared both qualitatively and quantitatively to the finite element model results. Validation criteria was set for the specimen-specific model data to be within two standard deviations of the experimental data. MANOVA with Brown-Forsythe post-hoc analysis was used to determine the significance of the change in average pressure, peak pressure, contact area, and contact force after opening the joint capsule. Statistical significance was set at $p < 0.05$. A power analysis was performed to determine our power with 3 specimens and the number of specimens that would be necessary for each measurement to achieve a target power of 80%. SAS was used for all of the statistical analyses.

3.4 Results

Quantitatively, model results were similar to experimental measures of average pressure and considerably smaller than experimental measures for contact area and peak pressure. Table 3.1 shows a summary of all the experimental and open joint capsule model data. Table 3.2 shows specimen-specific percent and absolute differences for the open joint capsule model and experimental measurements.

Table 3.1 Comparison of Tekscan (Tek) and model (Mod) data for all specimens, along with OA grades from the Eaton-Littler (E-L), Outerbridge (OB), and ICRS classification systems. The validation criterion (VC) of +/- 2 standard deviations of experimental data was included.

	AP (MPa)		PP (MPa)		CA (mm^2)		CF (N)		OA Grade		
Specimen	Tek	Mod	Tek	Mod	Tek	Mod	Tek	Mod	E-L	OB	ICRS
1	0.24	0.44	0.68	1.41	44	32	11	14*	1	3	2
2	0.33	0.50	0.76	2.78	55	29	18	14*	1	4	3c
3	0.29	0.52	1.03	2.43	58	16	17	8**	3	2	1b
VC	0.09		0.37		15		8				

*Data was within two standard deviations of the experimental data and met validation criteria

**Data was just outside of two standard deviations of experimental data and nearly met validation criteria

Model data for the average pressure and peak pressure not meet the validation criteria for any of the specimens. The model data for contact area did not meet the validation criteria for any of the specimens and was consistently smaller than the Tekscan data. Contact force data met the validation criteria for Specimens 1 and 2, and it was just outside the validation threshold for Specimen 3.

Table 3.2 Percentage and absolute difference comparison of Tekscan and Model data for all specimens

	AP (MPa)		PP (MPa)		CA (mm^2)		CF (N)	
Specimen	% Diff	Abs Diff	% Diff	Abs Diff	% Diff	Abs Diff	% Diff	Abs Diff
1	83	0.20	107	0.73	27	12	27	3
2	52	0.17	266	2.02	47	26	22	4
3	79	0.23	136	1.40	72	42	53	9

A filter was applied to experimental data to account for residual pressures and contact areas that were registered by the sensors without load. Table 3.3 illustrates the effect that applying the filter had on contact area, a fundamental value in Tekscan's measurement calculations.

Table 3.3 Comparison of Tekscan and model data for all specimens.

Specimen	Unfiltered CA (mm^2)	Filtered CA (mm^2)
1	102	44
2	112	55
3	65	58

Table 3.4 shows a summary of the intact and open joint capsule model contact measurements. Our power analysis reported a power of 0.68, 0.55, 0.59, and 0.93 for AP, PP, CA, and CF, respectively. To obtain a target power of 80%, 4, 6, and 5 samples are required for AP, PP, and CA respectively. Opening the joint capsule was shown to not have a significant effect on the

contact measurements ($p = 0.3559$). The results for Wilks' Lambda, Pillai's Trace, Hotelling-Lawley Trace, and Roy's Greatest Root were congruent for the MANOVA analysis.

Table 3.4 Comparison of model data for an intact joint capsule and open joint capsule

	AP (MPa)		PP (MPa)		CA (mm^2)		CF (N)	
Specimen	Intact	Open	Intact	Open	Intact	Open	Intact	Open
1	0.10	0.44	0.30	1.41	5	32	0.50	14
2	0.22	0.50	0.98	2.78	12	29	3	14
3	0.36	0.52	1.71	2.43	15	16	6	8

Per the model contact maps, contact location did not experience a noticeable shift after opening the joint capsule (Figure 3.3). Qualitatively, some correspondence for the location and relative size of contact between the experimental and model data for Specimens 1 and 2 was noticeable. Contact location on the metacarpal surface was similar for Specimens 1 and 3 but different for Specimen 2. The beak of the metacarpal in the modeling images was rotated approximately 20° to simulate the amount of pronation during key pinch [28]. This was done to aide qualitative comparisons between model and Tekscan pressure maps.

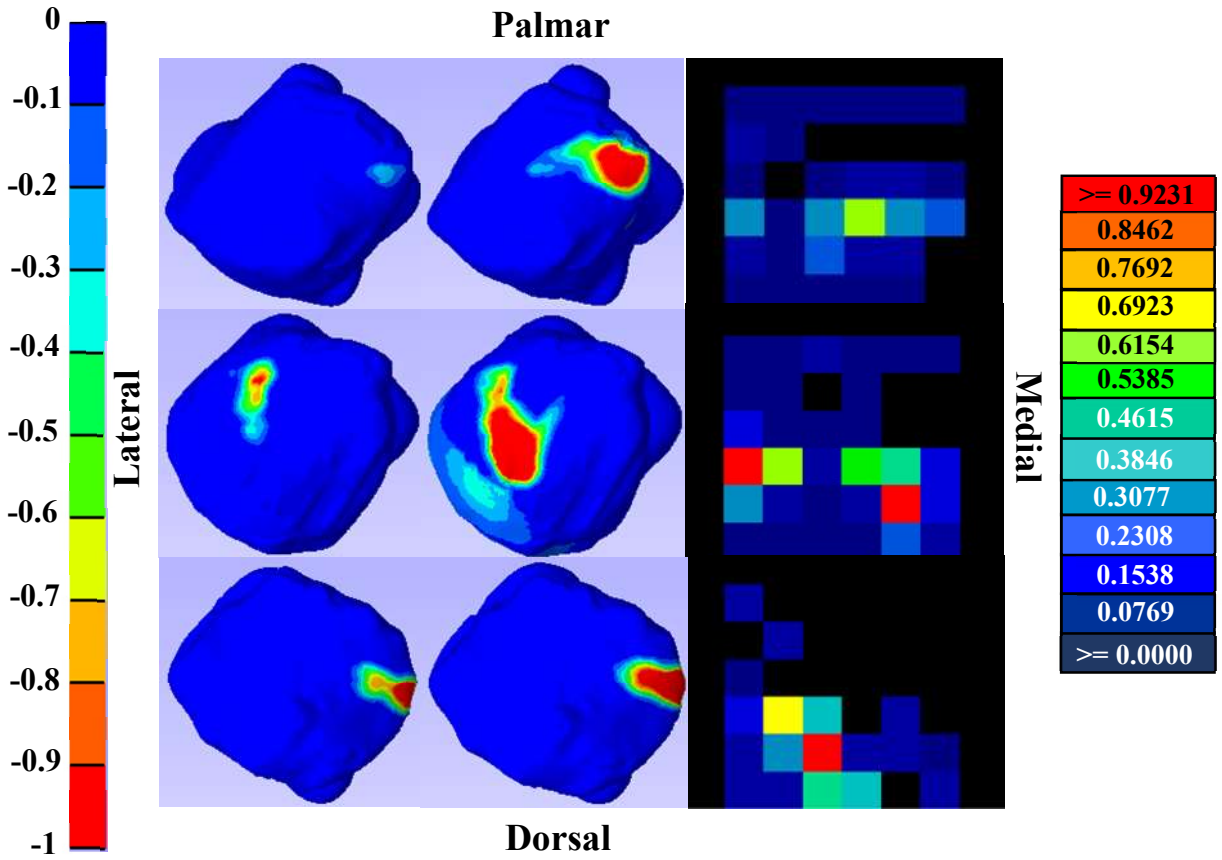

Figure 3.3 Contact model and Tekscan pressure (MPa) map comparisons. The top, middle, and bottom rows are Specimens 1, 2, and 3, respectively. The left, middle, and right columns illustrate the intact joint capsule contact model results, the open joint capsule contact model results, and the Tekscan (open capsule) experimental results, respectively. Contact area calculations from Tekscan data did not include the lowest pressure level.

3.5 Discussion

Pressure-sensitive Fuji films have previously been used to determine the location of contact within the basilar thumb joint during joint loading [8, 20, 29]. Tekscan pressure sensors are another common method used for biomechanical research because of their ability to record real-time dynamic data and avoid the issue of insertion artifact that can skew analysis of the experimental data. Past experiments have used Tekscan sensors for other joints such as the wrist [30], hip [31], knee [32], and ankle [33], that were designed for the analysis of that specific joint.

A Tekscan sensor has not been designed specifically for the thumb, so the Model 4201 wrist sensor was trimmed to fit within the joint and maximize coverage of the articular surface area.

The contact pressure magnitudes and locations were not consistent across all of the specimens, but a qualitative agreement between the two methods can be recognized after visual comparison of the individual experimental and model contact patterns. It must be noted that, while the sensors were consistently placed in the joint, inter-specimen variability could lead to slightly different orientations of each joint. A rotation of 20° was assumed to ease comparisons between the two pressure maps, but that may be too large or too little for each case and cause some disagreement. However, comparisons between the two pressure maps are only meant for qualitative, not quantitative, evaluation of the investigative methods. Another distinguishing detail for each comparison is that Specimen 3, which had the least favorable matchup between model and Tekscan pressure maps, had the most severe radiographic OA grade.

Each of the models only met the validation criteria, or came close to meeting the criteria, for contact force. Several factors have to be considered when interpreting the results and drawing conclusions for each of the contact measurement comparisons. By their nature, the Tekscan sensors register the amount of force that is applied and pressure outputs are calculated from the registered force and number of sensels that are activated. Therefore, it is not surprising to see that contact force met validation criteria for each specimen. A critical factor to consider for contact force measurements is effect of the packing tape used to prevent sensor contamination. The size of the sensing area and the modifications made to the sensor were influenced by two factors. The goal was to have a sensor area that provided maximum coverage of the joint surface while also maintaining a sufficient distance from the edge of the tape seal. This would effectively prevent fluids from entering the sensor and allow for its reuse in additional experiments. The results of

past iterations of this experiment revealed that packaging tape was more effective than other kinds of tape in preventing contamination. However, the packaging tape increased the sensor's stiffness. The increased stiffness of the sensor would affect its ability to conform to the joint surface during loading and could have caused the production of a pressure signal just through insertion of the sensor into the joint and its conforming to the articular surfaces. The sensitivity of the sensors (i.e. the gain) was increased to register smaller contact forces in the joint, but that had the effect of decreasing their measurement range without affecting our ability to measure peak pressure values. The increased sensitivity was necessary to provide better context when evaluating the experimental pressure maps and make comparisons with the model data possible. The greater stiffness and sensitivity also increased the likelihood that bending of the sensor within the joint during active loading would register small pressures and contact where none may be occurring. This is supported by our unfiltered contact area measurements of approximately 100 mm^2 in the first two specimens. Contact area of that magnitude is approximately two-thirds of the entire articular surface area [34, 35] and much larger than previously reported contact areas in the joint [15, 19, 29, 36], so it was determined that a filter was necessary. The small size of the joint and the curvature of the surfaces could have an effect on the sensor's output for contact area. Contact on only a portion of a sensel will cause the Tekscan software to consider the entire sensel area for calculations. This could cause an overestimation of contact area and register residual contact pressures on the joint surface. This observation may explain why experimental was consistently larger than the model contact area did not meet validation criteria for any of the specimens, and this observation is supported through the visual comparison of our experimental and model data. Tekscan uses contact area and the base sensel area of 3.63 mm^2 for all of its pressure calculations. Tekscan defines average pressure as the total force registered by

the sensors divided by the total area of the sensels in contact. This definition, along with an overestimation of area, could explain why the experimental average pressure values are smaller than the model data for each specimen. While peak pressure measurements may be affected by the sensor's sensitivity, it may feel a larger influence from the sensor's limitations in measuring contact area. The top 1% of pressure values from the model elements were averaged to define the peak pressure. Tekscan allows for the user to define the number of sensels to include in peak pressure measurements, and the average pressure is calculated on each frame of data using that input. An area of one sensel was used for determining peak pressure measurements from Tekscan data, but the base area unit of 3.63 mm^2 may still be an overestimation of the contact area where peak forces occur. There also exists the possibility that peak contact forces may be located such that the peak force is distributed over multiple sensels. Inclusion of multiple sensels in peak pressure measurements would further affect experimental peak pressure values. The only study that we found that used Tekscan sensors in the basilar thumb joint was performed by Cheema et al [19] who used completely intact Tekscan Model 6900 sensors. Their aim was to quantify the contact area and pressure within the basilar thumb joint during lateral pinch and how it changed after trapezial osteotomy. The Model 6900 used in their study has an increased sensel spatial resolution of 62.0 sensels/cm^2 as opposed to a spatial resolution of 27.6 sensels/cm^2 for the Model 4201. They reported mean contact area results of approximately 25.8 mm^2 in the specimens before an osteotomy, which is different from our reported experimental results but closer to our model results. Future validation studies could be performed with different sensors, such as a modified version of the Model 6900, to increase the number of sensors covering the articular surface area and allow for more precise calculations of contact area.

Our power analysis showed that three additional specimens are necessary to achieve sufficient power for all four contact measurements. The nature of cadaveric testing and the model creation process make working with larger numbers of specimens difficult. Due to the fact that three of our four contact measurements were underpowered, it would not be appropriate to draw conclusions about the significance of opening the joint capsule. However, the average pressure, peak pressure, contact force, and contact area all consistently trended upward after opening the joint capsule in each specimen. Visual inspection of the contact pattern results suggests that contact location may also be affected by opening the joint capsule. There have not been any previous studies that have examined the effect that opening the joint capsule has on the contact mechanics. Our results provide preliminary evidence that contact measurements may be affected but that the general nature of the contact is not substantially changed. This data, along with the inherent difficulty of performing completely accurate joint mechanics measurements in cadaveric experiments, underscore the usefulness of models to examine joint contact patterns and the need for their validation.

There is no one gold standard when it comes to validation criteria, largely due to the different types of outcome measures for various models. Several studies use statistical analyses and direct comparison of experimental and model data to draw correlations, but explicit validation criteria are not stated [32, 33, 37, 38]. Yet, without fail they declare the model validated. For the case of comparing differences in absolute magnitude of the data, because of the low absolute pressures, a small difference in measurements may translate to a sizable percentage difference and a failure to meet a set validation criterion. Such a case is observed with the average pressure for Specimen 1 whose had an absolute difference of 0.20 MPa between the model and Tekscan data but which amounted to a 83% difference.

The material properties assigned for the articular cartilage and bones of the specimen-specific model geometries is an important consideration. Linear elastic [30, 32, 33] and neo-hookean [36-39] material models are common constitutive models for articular cartilage in contact analyses. Under instantaneous loads cartilage acts as an incompressible solid so linear constitutive models can be considered adequate. However, cartilage experiences large in vivo deformations and exhibits a nonlinear stress-strain response, so hyperelastic constitutive models such as neo-hookean are more appropriate [23]. More complicated constitutive models such as linear biphasic, which account for the different contributions of the fluid within the cartilage and the collagen framework, are useful for applications such as analysis of the stress distribution through the cartilage thickness during dynamic loading. However, the primary consideration that dictates the appropriate constitutive model is the simplest model that accurately predicts the outcome of the pertinent measurements. Neo-hookean constitutive models are less complex and simpler to incorporate into contact models which makes them more suited for future clinical and large-scale research contact analyses. The literature on contact models for the basilar thumb joint is limited, but a few three-dimensional models have been used before to measure contact location during functional tasks. Joint space narrowing has been measured to determine the proximity of the metacarpal and trapezium surfaces and likely areas of increased contact [40, 41]. Finite element models have been used to determine the location of cartilage contact area and peak contact stress in the joint as well [20, 36]. However, none of these studies provided direct validation of the modeling technique. The literature concerning finite element models of the basilar thumb joint is limited. Neo-hookean constitutive models were used in our analysis due to their simplicity and to test their efficacy within our given model creation and analysis procedure. Shi et al performed a preliminary two-dimensional analysis of contact within the basilar thumb

joint using models created from four specimens to compare with experimental pressure patterns from Fuji film, and they found a close correlation between the two [20]. Schneider et al modeled the contact area and peak pressure locations in the basilar thumb joint during different functional tasks with the articular cartilage represented as a neo-hookean constitutive model [36]. They believed that more complex constitutive models of cartilage would not significantly change their contact results.

Element type has an effect on the contact analysis results as well. Linear tetrahedral elements are often used in contact mechanics due to the ease and robustness of automated meshing, and they have been used in some recent studies of articular contact in the wrist [26] and knee [42]. Linear tetrahedral elements have several issues that can affect their accuracy, such as the ability to only represent a constant strain across the element and thus necessitates fine discretizations and increased solution times, so hexahedral elements are more common in articular contact analyses despite the challenge of creating meshes for complex geometries [32, 33, 36-39]. Quadratic tetrahedral elements could also be utilized to maintain the advantages that a tetrahedral element mesh provides while representing curved boundaries more effectively [43]. Schneider et al used a custom template mesh to preserve articular surface boundaries of the joint surfaces and then extruded them to create a uniformly thick hexahedral mesh to represent the cartilage [36]. In the context of analyzing one or only a few specimens, more care and time can be taken to perform custom refinements of the articular mesh. Our segmentation and meshing software ScanIP allowed for easy automated generation and refinement of a linear tetrahedral mesh for the bone and cartilage which would be ideal for both clinical applications, where timely analyses are necessary, and in large studies where many subjects must be analyzed in a timely

manner as well. Therefore, it was appropriate to examine the linear tetrahedral mesh in the context of our model generation procedure.

There are several limitations that are associated with the use pressure-sensors and model creation. A validation criteria of two standard deviations of the experimental measures has been used before in joint modeling studies [30, 44]. The small number of specimens used in experiments such as ours, as well as the factors associated with data collection, could increase the standard deviations of experimental measures. This could make the validation boundaries too large and influence how many models and measurements fulfill validation criteria. Standard deviations were calculated across the specimens to establish the validation thresholds. Future experiments could record multiple trials for each specimen and determine standard deviations and validation thresholds for each model. However, the tendency of the sensor measurements to creep over time (even under ideal conditions of load control) and with repeated use could skew the data. Another difficulty with collecting multiple measurements is the placement of the sensor. Replicating the exact orientation and position of a sensor for each trial is difficult, so some error will be present when combining data over multiple trials. The experimental data recorded was collected as soon as the load was applied to avoid creep, and the model data was the result of prolonged loading during the 3.25 minute scan. Possibly due to the concern of sensor creep several studies also only recorded one trial of experimental data [32, 33] or only used the first trial for data analysis [30]. An average of the data over multiple trials was also used to account for creep from the sensors [44]. Tekscan and other pressure-sensitive sensors measure the force on the cartilage surface [45], so the differences in the amount of relaxation of the cartilage between the experimental and modeling conditions, as well as the effects of the sensors in the joint, could have produced some differences between the model and experimental data.

The cadaveric specimens were kept in frozen storage before the experiments and had to be thawed before experimentation. Exposure to conditions at room temperature during the 4 hour experimental timeframe could have caused some deterioration of specimen tissues. This could have affected the material properties of all the soft tissues and their response while simulating key pinch.

The type of calibration and the surface that is used to calibrate the sensor can also have an effect on the results. Linear calibrations are considered suitable over a limited loading range whereas two-point power calibrations are considered suitable for loading scenarios that have a large variance in load magnitude [46]. Power calibrations were chosen for our experiments, but future experiments could also apply linear or custom calibrations as well. Tekscan offers a rule of thumb that calibration points for power calibrations should be 20% and 80% of the expected maximum test load. However, selecting calibration points that do not fit Tekscan's recommendations could not be avoided given the equipment available. The maximum pressure PB100E calibration device can apply is 100 psi. This is well below the estimated peak contact pressure of 140 psi (0.96 MPa) [8]. The appeal of a calibration device such as the PB100E and its corresponding software is the simplicity and ability to quickly calibrate multiple sensors. Further experiments could utilize other mechanical testing systems that are able to apply larger pressure loads. It is recommended to calibrate sensors on a surface that is identical to the experimental surface, but the unique shape of the joint surface is difficult to replicate for calibration purposes. The size and shape of the bones may have impacted the model contact results as well.

3.6 Conclusions/Future Work

The depth of literature regarding models that describe basilar thumb joint contact mechanics is limited, and within that context our validation study for the basilar thumb joint and

its results appear to be a novel addition. Direct measurement of contact locations and stresses in the basilar thumb joint are difficult due to its size and curved articular surfaces, but nonetheless direct validation of models against experimental data will provide the strongest support for the use of three-dimensional finite element models within future research and clinical applications. The joint capsule was disrupted to enable the insertion of a Tekscan pressure-sensitive sensor into the joint. This action may have a significant effect on the in vivo joint contact mechanics. However, our results indicate that contact measurements were not significantly affected. Future validation studies could mimic the insertion of a sensor into the joint space and examine its impact on contact mechanics with our modeling method. The validation of pressure measurements still remains a challenge, but our results support that the modeling technique could be used to determine general contact locations and to track its progression across the joint surface in a longitudinal study. Since there is not a specific pressure-sensitive sensor designed for the basilar thumb joint, an important choice for future direct validation experiments is to determine a more appropriate sensor. This would enhance the ability to accurately record the contact area and thus lead to better pressure measurements. Finite element models discretizing the articular cartilage using hexahedral or quadratic tetrahedral elements could also be used in future validation studies. While there was not any statistical significance, opening of the joint capsule appeared to affect the contact measurements. This further emphasizes the need for appropriate validation and use of computational modeling to understand in vivo conditions.

3.7 References

1. Dahaghin, S., S.M. Bierma-Zeinstra, A.Z. Ginai, H.A. Pols, J.M. Hazes, and B.W. Koes, *Prevalence and pattern of radiographic hand osteoarthritis and association with pain and disability (the Rotterdam study).* Ann Rheum Dis, 2005. **64**(5): p. 682-7.

2. Wilder, F.V., J.P. Barrett, and E.J. Farina, *Joint-specific prevalence of osteoarthritis of the hand.* Osteoarthritis Cartilage, 2006. **14**(9): p. 953-7.

3. Armstrong, A.L., J.B. Hunter, and T.R. Davis, *The prevalence of degenerative arthritis of the base of the thumb in post-menopausal women.* J Hand Surg Br, 1994. **19**(3): p. 340-1.

4. Andriacchi, T.P., A. Mundermann, R.L. Smith, E.J. Alexander, C.O. Dyrby, and S. Koo, *A framework for the in vivo pathomechanics of osteoarthritis at the knee.* Ann Biomed Eng, 2004. **32**(3): p. 447-57.

5. Arokoski, J.P., J.S. Jurvelin, U. Vaatainen, and H.J. Helminen, *Normal and pathological adaptations of articular cartilage to joint loading.* Scand J Med Sci Sports, 2000. **10**(4): p. 186-98.

6. Doerschuk, S.H., D.G. Hicks, V.M. Chinchilli, and V.D. Pellegrini, Jr., *Histopathology of the palmar beak ligament in trapeziometacarpal osteoarthritis.* J Hand Surg Am, 1999. **24**(3): p. 496-504.

7. Imaeda, T., G. Niebur, K.N. An, and W.P. Cooney, 3rd, *Kinematics of the trapeziometacarpal joint after sectioning of ligaments.* J Orthop Res, 1994. **12**(2): p. 205-10.

8. Pellegrini, V.D., Jr., C.W. Olcott, and G. Hollenberg, *Contact patterns in the trapeziometacarpal joint: the role of the palmar beak ligament.* J Hand Surg Am, 1993. **18**(2): p. 238-44.

9. Van Brenk, B., R.R. Richards, M.B. Mackay, and E.L. Boynton, *A biomechanical assessment of ligaments preventing dorsoradial subluxation of the trapeziometacarpal joint.* J Hand Surg Am, 1998. **23**(4): p. 607-11.

10. Pelligrini, V.D., Jr., *Osteoarthritis of the trapeziometacarpal joint: the pathophysiology of articular cartilage degeneration. II. Articular wear patterns in the osteoarthritic joint.* J Hand Surg Am, 1991. **16**(6): p. 975-82.

11. Eaton, R.G. and S.Z. Glickel, *Trapeziometacarpal osteoarthritis. Staging as a rationale for treatment.* Hand Clin, 1987. **3**(4): p. 455-71.

12. Koebke, J. and W. Thomas, *[Biomechanical investigations on the aetiology of arthrosis of the first carpometacarpal joint (author's transl)].* Z Orthop Ihre Grenzgeb, 1979. **117**(6): p. 988-94.

13. Menon, J., *The problem of trapeziometacarpal degenerative arthritis.* Clin Orthop Relat Res, 1983(175): p. 155-65.

14. Momose, T., Y. Nakatsuchi, and S. Saitoh, *Contact area of the trapeziometacarpal joint.* J Hand Surg Am, 1999. **24**(3): p. 491-5.

15. Ateshian, G.A., J.W. Ark, M.P. Rosenwasser, R.J. Pawluk, L.J. Soslowsky, and V.C. Mow, *Contact areas in the thumb carpometacarpal joint.* J Orthop Res, 1995. **13**(3): p. 450-8.

16. Cohen, Z.A., J.H. Henry, D.M. McCarthy, V.C. Mow, and G.A. Ateshian, *Computer simulations of patellofemoral joint surgery. Patient-specific models for tuberosity transfer.* Am J Sports Med, 2003. **31**(1): p. 87-98.

17. Pillai, R.R., B. Thoomukuntla, G.A. Ateshian, and K.J. Fischer, *MRI-based modeling for evaluation of in vivo contact mechanics in the human wrist during active light grasp.* J Biomech, 2007. **40**(12): p. 2781-7.

18. Majima, M., E. Horii, H. Matsuki, H. Hirata, and E. Genda, *Load transmission through the wrist in the extended position.* J Hand Surg Am, 2008. **33**(2): p. 182-8.

19. Cheema, T., C. Salas, N. Morrell, L. Lansing, M.M. Reda Taha, and D. Mercer, *Opening wedge trapezial osteotomy as possible treatment for early trapeziometacarpal osteoarthritis: a biomechanical investigation of radial subluxation, contact area, and contact pressure.* J Hand Surg Am, 2012. **37**(4): p. 699-705.

20. Shi, Q., H. Hashizume, H. Inoue, T. Miyake, and N. Nagayama, *Finite element analysis of pathogenesis of osteoarthritis in the first carpometacarpal joint.* Acta Med Okayama, 1995. **49**(1): p. 43-51.

21. Jafari, A., F. Farahmand, and A. Meghdari, *A rigid body spring model to investigate the lateral shift - restraining force behavior of the patella.* Conf Proc IEEE Eng Med Biol Soc, 2007. **2007**: p. 4679-82.

22. Fernandez, J.W. and M.G. Pandy, *Integrating modelling and experiments to assess dynamic musculoskeletal function in humans.* Exp Physiol, 2006. **91**(2): p. 371-82.

23. Henak, C.R., A.E. Anderson, and J.A. Weiss, *Subject-specific analysis of joint contact mechanics: application to the study of osteoarthritis and surgical planning.* J Biomech Eng, 2013. **135**(2): p. 021003.

24. Henninger, H.B., S.P. Reese, A.E. Anderson, and J.A. Weiss, *Validation of computational models in biomechanics.* Proc Inst Mech Eng H, 2010. **224**(7): p. 801-12.

25. Maas, S.A., B.J. Ellis, G.A. Ateshian, and J.A. Weiss, *FEBio: finite elements for biomechanics.* J Biomech Eng, 2012. **134**(1): p. 011005.

26. Johnson, J.E., P. Lee, T.E. McIff, E.B. Toby, and K.J. Fischer, *Computationally efficient magnetic resonance imaging based surface contact modeling as a tool to evaluate joint injuries and outcomes of surgical interventions compared to finite element modeling.* J Biomech Eng, 2014. **136**(4).

27. Kumar, R., D.M. Pierce, V. Isaksen, C.L. Davies, J.O. Drogset, and M.B. Lilledahl, *Comparison of Compressive Stress-Relaxation Behavior in Osteoarthritic (ICRS Graded) Human Articular Cartilage.* Int J Mol Sci, 2018. **19**(2).

28. Cooney, W.P., 3rd, M.J. Lucca, E.Y. Chao, and R.L. Linscheid, *The kinesiology of the thumb trapeziometacarpal joint.* J Bone Joint Surg Am, 1981. **63**(9): p. 1371-81.

29. Cullen, J.P., M.A. Parentis, V.M. Chinchilli, and V.D. Pellegrini, Jr., *Simulated Bennett fracture treated with closed reduction and percutaneous pinning. A biomechanical analysis of residual incongruity of the joint.* J Bone Joint Surg Am, 1997. **79**(3): p. 413-20.

30. Fischer, K.J., J.E. Johnson, A.J. Waller, T.E. McIff, E.B. Toby, and M. Bilgen, *MRI-based modeling for radiocarpal joint mechanics: validation criteria and results for four specimen-specific models.* J Biomech Eng, 2011. **133**(10): p. 101004.

31. Townsend, K.C., H.D. Thomas-Aitken, M.J. Rudert, A.M. Kern, M.C. Willey, D.D. Anderson, and J.E. Goetz, *Discrete element analysis is a valid method for computing joint contact stress in the hip before and after acetabular fracture.* J Biomech, 2018. **67**: p. 9-17.

32. Kiapour, A., A.M. Kiapour, V. Kaul, C.E. Quatman, S.C. Wordeman, T.E. Hewett, C.K. Demetropoulos, and V.K. Goel, *Finite element model of the knee for investigation of injury mechanisms: development and validation.* J Biomech Eng, 2014. **136**(1): p. 011002.

33. Anderson, D.D., J.K. Goldsworthy, W. Li, M. James Rudert, Y. Tochigi, and T.D. Brown, *Physical validation of a patient-specific contact finite element model of the ankle.* J Biomech, 2007. **40**(8): p. 1662-9.

34. Halilaj, E., D.C. Moore, D.H. Laidlaw, C.J. Got, A.P. Weiss, A.L. Ladd, and J.J. Crisco, *The morphology of the thumb carpometacarpal joint does not differ between men and women, but changes with aging and early osteoarthritis.* J Biomech, 2014. **47**(11): p. 2709-14.

35. Halilaj, E., M.J. Rainbow, C.J. Got, D.C. Moore, and J.J. Crisco, *A thumb carpometacarpal joint coordinate system based on articular surface geometry.* J Biomech, 2013. **46**(5): p. 1031-4.

36. Schneider, M.T.Y., J. Zhang, J.J. Crisco, A.C. Weiss, A.L. Ladd, K. Mithraratne, P. Nielsen, and T. Besier, *Trapeziometacarpal joint contact varies between men and women during three isometric functional tasks.* Med Eng Phys, 2017. **50**: p. 43-49.

37. Anderson, A.E., B.J. Ellis, S.A. Maas, C.L. Peters, and J.A. Weiss, *Validation of finite element predictions of cartilage contact pressure in the human hip joint.* J Biomech Eng, 2008. **130**(5): p. 051008.

38. Henak, C.R., A.L. Kapron, A.E. Anderson, B.J. Ellis, S.A. Maas, and J.A. Weiss, *Specimen-specific predictions of contact stress under physiological loading in the human hip: validation and sensitivity studies.* Biomech Model Mechanobiol, 2014. **13**(2): p. 387-400.

39. Buchler, P., N.A. Ramaniraka, L.R. Rakotomanana, J.P. Iannotti, and A. Farron, *A finite element model of the shoulder: application to the comparison of normal and osteoarthritic joints.* Clin Biomech (Bristol, Avon), 2002. **17**(9-10): p. 630-9.

40. D'Agostino, P., B. Dourthe, F. Kerkhof, G. Harry Van Lenthe, F. Stockmans, and E.E. Vereecke, *In vivo biomechanical behavior of the trapeziometacarpal joint in healthy and osteoarthritic subjects.* Clin Biomech (Bristol, Avon), 2017. **49**: p. 119-127.

41. Halilaj, E., D.C. Moore, T.K. Patel, D.H. Laidlaw, A.L. Ladd, A.P. Weiss, and J.J. Crisco, *Older asymptomatic women exhibit patterns of thumb carpometacarpal joint space narrowing that precede changes associated with early osteoarthritis.* J Biomech, 2015. **48**(13): p. 3634-40.

42. McErlain, D.D., J.S. Milner, T.G. Ivanov, L. Jencikova-Celerin, S.I. Pollmann, and D.W. Holdsworth, *Subchondral cysts create increased intra-osseous stress in early knee OA: A finite element analysis using simulated lesions.* Bone, 2011. **48**(3): p. 639-46.

43. Maas, S.A., B.J. Ellis, D.S. Rawlins, and J.A. Weiss, *Finite element simulation of articular contact mechanics with quadratic tetrahedral elements.* J Biomech, 2016. **49**(5): p. 659-667.

44. Johnson, J.E., T.E. McIff, P. Lee, E.B. Toby, and K.J. Fischer, *Validation of radiocarpal joint contact models based on images from a clinical MRI scanner.* Comput Methods Biomech Biomed Engin, 2014. **17**(4): p. 378-87.

45. Ateshian, G.A., W.M. Lai, W.B. Zhu, and V.C. Mow, *An asymptotic solution for the contact of two biphasic cartilage layers.* J Biomech, 1994. **27**(11): p. 1347-60.

46. Brimacombe, J.M., D.R. Wilson, A.J. Hodgson, K.C. Ho, and C. Anglin, *Effect of calibration method on Tekscan sensor accuracy.* J Biomech Eng, 2009. **131**(3): p. 034503.

Chapter 4. Conclusions and Future Directions

The anteroposterior (AP) view of the joint was shown to provide the best view of metacarpal lateral subluxation during simulated key pinch. It was also shown that the amount of lateral subluxation had a significant correlation with the radiographic Eaton-Littler stage but did not have a significant correlation with the more robust visual Outerbridge or ICRS classifications. Sectioning of the anterior oblique ligament (AOL) did not have a significant effect on the lateral subluxation. However, the specimens that were used in our experiments had an advanced age at time of death (average = 72 years, range = 54-88 years). Six of the eleven specimens were found to have advanced OA with a grade 3 or 4 for both of the visual classification systems. Osteoarthritic changes to the joint could affect the amount of subluxation measured after the AOL is transected. Comparison of the model and Tekscan experimental data showed that the quantitative measurements of contact area, average pressure, and peak pressure did not meet the validation criteria for any of the specimens. Contact force met validation criteria in two of the three specimens and was just outside of validation range for the third specimen. Tekscan measurements appeared to overestimate contact area for all three specimens due to low resolution and warping of the sensor to fit into the joint. This apparent overestimation most likely also contributed to the average pressure measurements not meeting validation criteria. Qualitative analysis of the contact patterns suggests that this modeling technique could be used to establish general contact locations and hotspots of increased contact pressure. The contact area, average pressure, peak pressure, and contact force were not significantly affected by opening the joint capsule. However, our statistical power was only above 80% for the contact force measure. Doubling the number of specimens, for a total of six specimens, for similar future studies should increase the statistical power to satisfactory levels for all four measurements.

Ligamentous laxity is believed to be a major contributor to the development of osteoarthritis (OA). Imaging is a valuable tool used in the OA diagnostic process that can be used to evaluate the laxity/instability of the joint. Stress radiographs can be used to visually inspect and quantify the joint instability to gain an understanding of the severity of OA, and this information is used to help guide future treatments. The AP view was found to provide the best view of the maximum amount of lateral subluxation. Consistency between physicians and researchers for the imaging angle used to evaluate the joint might lead to more agreement between them about the advancement of the disease, the role of subluxation in the diagnostic process, as well as more uniform treatments. The AOL, along with the dorsoradial ligament (DRL), is thought to be one of the major stabilizers of the joint that prevents dorsal subluxation of the metacarpal. Common functional tasks, such as key pinch and grasp, place these ligaments under different strains. We measured lateral subluxation before and after the AOL was transected to provide further clarity for its role in the joint's stability during key pinch. Our results did not show significant changes in lateral subluxation after the AOL was transected, but the advanced age of the specimens could have influenced the results. Additional investigations that transect the DRL under similar experimental conditions would be necessary to make any comparisons about its role and the AOL's role in preventing lateral subluxation during key pinch. The AOL is likely still a very important stabilizer during other functional tasks. Three-dimensional models used with analytic methods such as the finite element method (FEM) are a powerful and less invasive tool to analyze joint contact mechanics. In order for these methods to garner trust that they will produce accurate predictions, they must be validated through comparisons to experimental data. Direct validation, which entails comparisons of specimen-specific experimental and model results, is the preferable method. There is not one gold standard for validation criteria, so as more

validation studies are performed the validation criteria and the experimental methods used to collect data for comparison may evolve. Model boundary conditions, constitutive material models for the organic tissues, and the types of elements that are used must each be carefully considered and selected to provide the simplest model conditions that will achieve accurate results.

Future work can be done to enhance our knowledge about the role of the AOL and other ligaments in preventing subluxation of the metacarpal. A similar study using simulated key pinch could be performed with a focus on the DRL and analyzing lateral subluxation. This could help to further define the DRL's role during key pinch. Subluxation in other simulated functional tasks such as jar grasp or jar twist could be performed as well. Different functional tasks are believed to place different strains on the supporting ligaments and thus lead to differential wear, so analyses of lateral subluxation during different functional tasks could further define the overall role and recruitment patterns of the AOL and the DRL. Future work can also be done to enhance validation studies of the basilar thumb joint. Sensors that have higher sensel resolution, such as the Model 6900, could possibly be used to reduce the overestimation of contact area. This would improve the comparison of the pressure measurements to model data and improve qualitative comparisons between the model and Tekscan contact locations. A pressure-sensitive sensor has not been designed specifically for the basilar thumb joint. Currently, sensors designed for other joints must be modified for experimental analysis of contact mechanics in the basilar thumb joint. If a sensor is trimmed, tape is necessary to provide a seal to prevent contamination of these sensors during experiments because modifications to the sensor area leave the edges of the sensor open to the environment. Given the frequency and severity of OA in the basilar thumb joint, projects to design and create a pressure-sensitive specifically for the basilar thumb joint

would be of great benefit for experimental and model validation studies. More proper sensors and experimental equipment for measuring contact mechanics in the basilar thumb joint would lead to more accurate pressure data and could directly lead to direct validation of computational modeling techniques. We only examined the effect that opening the joint capsule had on contact mechanics, but the additional step of inserting a plastic film or sheet to replicate the presence of a pressure-sensitive film could also be analyzed to determine its impact. Less invasive computational analytic methods for understanding the joint could potentially lead to a greater understanding of OA and contribute to future treatments. For models using FEM, the goal when specifying model criteria is generally to select the simplest parameters that will provide accurate results. Further analysis of the effect of element type on accuracy and computation time could be performed in future validation studies. The use of linear tetrahedral elements allows for automated and simple meshing, but more elements are needed. Hexahedral elements are commonly used in articular contact analyses but can require much more manual work to create adequate element meshes. Quadratic tetrahedral elements provide the same meshing advantages of linear tetrahedral elements while also being able to represent curved boundaries more effectively. Comparisons of computation time, accuracy of the contact results when compared to experimental data, and the complexity/difficulty of mesh generation, such as that reported by Maas et al for the hip [1], would be useful for determining appropriate modeling parameters for research studies and clinical applications focused on smaller joints like the basilar thumb joint.

Reference

1. Maas, S.A., B.J. Ellis, D.S. Rawlins, and J.A. Weiss, *Finite element simulation of articular contact mechanics with quadratic tetrahedral elements.* J Biomech, 2016. **49**(5): p. 659-667.

Appendix

Linear Regression – Subluxation vs. OA Grade

```
*Read the data file into SAS*;
data Grading_stats;
      input Subluxation Radiographic Visual_ICRS1 Visual_ICRS2
Visual_Outerbridge;
      cards;
      42.52078 4 2 1 2
      20.23701 2 1 1 1
      22.32060 2 4 3 3
      38.54801 3 8 4 4
      21.70139 2 4 3 3
      38.83258 3 4 3 3
      60.29743 4 8 4 4
      15.43876 1 3 2 3
      11.46266 1 6 3 4
      51.59551 3 2 1 2
      25.94645 1 2 1 2
      ;

*Regression analysis for ICRS1 rating*;
proc reg data = Grading_stats;
      model Visual_ICRS1=Subluxation;
      output out = CheckFit1 predicted = y_hat1 residual = res1;
run;
/* normal probability plot */
proc univariate data = CheckFit1 normal plot;
      var res1;
run;
/* residuals vs. predicted plot (check for variance assumption)*/
proc sgplot data = CheckFit1;
      scatter y = res1 x = y_hat1;
run;

*Regression analysis for ICRS2 rating*;
proc reg data = Grading_stats;
      model Visual_ICRS2=Subluxation;
      output out = CheckFit2 predicted = y_hat2 residual = res2;
run;
/* normal probability plot */
proc univariate data = CheckFit2 normal plot;
      var res2;
run;
/* residuals vs. predicted plot (check for variance assumption)*/
proc sgplot data = CheckFit2;
      scatter y = res2 x = y_hat2;
run;

*Regression analysis for Outerbridge rating*;
proc reg data = Grading_stats;
      model Visual_Outerbridge=Subluxation;
      output out = CheckFit3 predicted = y_hat3 residual = res3;
run;
/* normal probability plot */
```

```
proc univariate data = CheckFit3 normal plot;
      var res3;
run;
/* residuals vs. predicted plot (check for variance assumption)*/
proc sgplot data = CheckFit3;
      scatter y = res3 x = y_hat3;
run;

*Regression analysis for radiographic rating*;
proc reg data = Grading_stats;
      model Radiographic=Subluxation;
      output out = CheckFit4 predicted = y_hat4 residual = res4;
run;
/* normal probability plot */
proc univariate data = CheckFit4 normal plot;
      var res4;
run;
/* residuals vs. predicted plot (check for variance assumption)*/
proc sgplot data = CheckFit4;
      scatter y = res4 x = y_hat4;
run;
```

Repeated Measures ANOVA – Subluxation Comparisons

```
*Input the data*;
data ThumbStudy;
      input specimen percent_sub1 percent_sub2 percent_sub3;
      cards;
      1 42.5207756 44.86193 40.94955
      2 20.23701 27.0676692 24.6569814
      3 22.3205965 24.5317497 24.5176471
      4 38.5480094 34.3235832 34.0139211
      5 21.7013889 20.2265372 22.1352711
      6 38.832576 40.2153732 41.7397661
      7 60.2974313 59.2637055 65.2403592
      8 15.4387612 42.4009234 18.1659389
      9 11.4626556 7.08186841 11.4253394
      10 51.5955056 64.7845468 62.1687929
      11 25.9464451 24.1013825 28.3061594
      ;

proc means data = ThumbStudy n mean std;
class specimen;
var percent_sub1 percent_sub2 percent_sub3;
run;

/* repeated measures ANOVA */
proc glm data = ThumbStudy;
      class specimen;
      model percent_sub1 - percent_sub3 = / ;
      *means specimen/ tukey;
        repeated sub 3 (1 2 3);
        output out = CheckFit predicted = y_hat residual = e_ijk;
run;
/* normal probability plot */
proc univariate data = CheckFit normal plot;
      var e_ijk;
run;
/* residuals vs. predicted plot (check for variance assumption)*/
proc sgplot data = CheckFit;
      scatter y = e_ijk x = y_hat;
run;
```

MANOVA – Intact Joint Capsule vs. Open Joint Capsule Contact Measurements

```
*Input the data*;
data ThumbStudy;
      input specimen group AP PP CA CF ;
      cards;
      1 1 0.0961 0.2997 5.07993 0.48818
      1 2 0.4383 1.4065 31.8958 13.9799
      2 1 0.2234 0.9762 12.0469 2.6912
      2 2 0.4998 2.7803 28.982 14.4852
      3 1 0.3636 1.7097 15.403 5.6005
      3 2 0.519 2.4301 16.2935 8.4563
      ;

proc means data = ThumbStudy;
      var AP PP CA CF;
run;

proc freq data = ThumbStudy;
      table group;
run;

proc sort data = ThumbStudy;
      by group;
run;

proc means data = ThumbStudy;
      by group;
      var AP PP CA CF;
run;

/* MANOVA */
proc glm data = ThumbStudy;
      class group;
      model AP PP CA CF = group ;
      manova h = group;
        output out = CheckFit predicted = y_hat residual = e_ijk;
run;
/* normal probability plot */
proc univariate data = CheckFit normal plot;
      var e_ijk;
run;
/* residuals vs. predicted plot (check for variance assumption)*/
proc sgplot data = CheckFit;
      scatter y = e_ijk x = y_hat;
run;
```

MATLAB Code for Experimental Data Filtering

```
%% File Notes and Purpose
%Author: Nolan Norton
%University of Kansas Bioengineering
%Created: March/April 2018
%Version number: 1
%Purpose: Threshold experimental data from Tekscan for joint pressure and
%contact area measurements. Updated pressure maps will also be created based
on the threshold value.
%Input Data Format: The imported data should be in an excel file in cells
A1:F6 and
%each frame should be written in a seperate tab.

%% Reading the data and Calculations

specimen_name = {'11845' '11725L' '11725R' '12300' '12551L' '12551R' '12053'
'11679' '11903' '12502'};  %created a cell array to be able to reference the
entire string within a cell
condition = {'Intact_Beak_Ligament' 'Cut_Beak_Ligament'};
global threshold;
threshold = input('What threshold for pressure (in MPa) values should be
applied? \n'); %Allows the user to input different threshold values for the
data.
for i = 1:1 %Just the first condition(for plotting reasons, probably could
rewrite to eliminate the outer loop)
    for j = 1:10  %Number of specimens
        for k = 1:10  %Number of frames per specimen
            fname = ['Specimen_' specimen_name{j} '_' condition{i}];
%Creating a string that will match the names of all of the excel files,
changes with each run. Had to use {} because of the previous cell array.
            tab = k;  %This will loop for the excel tabs that contain numbers
for each slide
            data = xlsread(fname, tab, 'A1:F6'); %Reads the data from the
excel sheet and tab for the specified run

[Contact_Area{i}(j,k),Average_Pressure{i}(j,k),Average_Force{i}(j,k),Peak_Pre
ssure{i}(j,k)] = parameter_calculation(data); %Calculations using a
subfunction and storing the values in matrices for later manipulation

            %Creating an updated plot after the data is thresholded
            %Black Markers
            black_logic = data < threshold;
            [black_row, black_col] = find(black_logic);
            %Blue Markers
            blue_logic = data >= threshold & data < 2/3; %This creates a
matrix with 1's in all of the places that meet the specified range and 0's
everywhere else. Why does it do this? Because this is a logical statement and
not an IF statement we only use one & to do an AND comparison.
            [blue_row, blue_col] = find(blue_logic); %Finds the row and
column (indices) of the nonzero elements and puts them into two column
vectors
            %Red Markers
            red_logic = data >= 2/3;
```

```
            [red_row, red_col] = find(red_logic); %The row vector goes by
columns and displays all of the rows that have a one (starting at the top).
The column vector counts how many times a 1 appears in the column.

            figure(j)
            subplot(2,5,k) %Creates a subplot of the graphs that add in the
first pane in the first row and then go from left to right
            name = [specimen_name{j} ' IBL'];


plot(black_col,black_row,'s','MarkerEdgeColor','k','MarkerFaceColor','k','Mar
kerSize',12); hold on;
            text(1.5,-0.15,name); %Adds text to make indentification of the
plots easier

plot(blue_col,blue_row,'s','MarkerEdgeColor','b','MarkerFaceColor','b','Marke
rSize',12); hold on;
            text(1.5,-0.15,name);

plot(red_col,red_row,'s','MarkerEdgeColor','r','MarkerFaceColor','r','MarkerS
ize',12); hold off;
            text(1.5,-0.15,name);
            xlim([1 6]); %Sets the x-axis values from 1 to 6
            ylim([1 6]);

            clear data;  %This clears the variable "data" that was originally
read from excel, but this may not be totally necessary because when the loop
is run again the variable "data" will be overwritten.
        end
    end
end
%The above for loop calculated the values for each slide for the intact beak
ligament specimens and put them into
%matrices that will be used to calculate overall averages.

i=2;
while i <= 2 %Just the second condition(for plotting reasons)
    j=1;
    while j <= 10
        k=1;
        while k <= 10
            fname = ['Specimen_' specimen_name{j} '_' condition{i}];
            tab = k;
            data = xlsread(fname, tab, 'A1:F6');

[Contact_Area{i}(j,k),Average_Pressure{i}(j,k),Average_Force{i}(j,k),Peak_Pre
ssure{i}(j,k)] = parameter_calculation(data); %Calculations using a
subfunction and storing the values in matrices for later manipulation

            %Creating an updated plot after the data is thresholded
            black_logic = data < threshold;
            [black_row, black_col] = find(black_logic);
            %Blue Markers
            blue_logic = data >= threshold & data < 2/3;
            [blue_row, blue_col] = find(blue_logic);
            %Red Markers
```

```
            red_logic = data >= 2/3;
            [red_row, red_col] = find(red_logic);

            figure(j+10) %Include the +10 so that the previous figures don't
get overwritten
            name = [specimen_name{j} ' CBL'];

            subplot(2,5,k)

plot(black_col,black_row,'s','MarkerEdgeColor','k','MarkerFaceColor','k','Mar
kerSize',12); hold on;
            text(1.5,-0.15,name);

plot(blue_col,blue_row,'s','MarkerEdgeColor','b','MarkerFaceColor','b','Marke
rSize',12); hold on;
            text(1.5,-0.15,name);

plot(red_col,red_row,'s','MarkerEdgeColor','r','MarkerFaceColor','r','MarkerS
ize',12); hold off;
            text(1.5,-0.15,name);
            xlim([1 6]);
            ylim([1 6]);

            clear data;
            k=k+1;
        end
        j=j+1;
    end
    i=i+1;
end
%The above for loop calculated the values for each slide for the cut beak
ligament specimens and put them into
%matrices that will be used to calculate overall averages.


%% Creating the Excel File

%Deleting the first row of each matrix
Contact_Area{1}(:,1) = [];
Average_Pressure{1}(:,1) = [];
Peak_Pressure{1}(:,1) = [];
Average_Force{1}(:,1) = [];

Contact_Area{2}(:,1) = [];
Average_Pressure{2}(:,1) = [];
Peak_Pressure{2}(:,1) = [];
Average_Force{2}(:,1) = [];

%Transposing each matrix so that each specimen's data is in the same column
Contact_Area{1} = Contact_Area{1}';
Average_Pressure{1} = Average_Pressure{1}';
Peak_Pressure{1} = Peak_Pressure{1}';
Average_Force{1} = Average_Force{1}';

Contact_Area{2} = Contact_Area{2}';
```

```
Average_Pressure{2} = Average_Pressure{2}';
Peak_Pressure{2} = Peak_Pressure{2}';
Average_Force{2} = Average_Force{2}';

%The averages of each column and specimen are calculated to compare to the
%models. This is a row array.
CA_mean_Intact = mean(Contact_Area{1});
AP_mean_Intact = mean(Average_Pressure{1});
PP_mean_Intact = mean(Peak_Pressure{1});
AF_mean_Intact = mean(Average_Force{1});

CA_mean_Cut = mean(Contact_Area{2});
AP_mean_Cut = mean(Average_Pressure{2});
PP_mean_Cut = mean(Peak_Pressure{2});
AF_mean_Cut = mean(Average_Force{2});

%Making the results column arrays
CA_mean_Intact = CA_mean_Intact';
AP_mean_Intact = AP_mean_Intact';
PP_mean_Intact = PP_mean_Intact';
AF_mean_Intact = AF_mean_Intact';

CA_mean_Cut = CA_mean_Cut';
AP_mean_Cut = AP_mean_Cut';
PP_mean_Cut = PP_mean_Cut';
AF_mean_Cut = AF_mean_Cut';

%Displaying the results
row_headers = {'Specimen 11845'; 'Specimen 11725L'; 'Specimen 11725R';
'Specimen 12300'; 'Specimen 12551L'; 'Specimen 12551R'; 'Specimen 12053';
'Specimen 11679'; 'Specimen 11903'; 'Specimen 12502'}; %Headers for the
columns
column_headers = {'Specimen Name' 'Intact Beak Ligament' 'Cut Beak
Ligament'};
Excel_title = 'Threshold Results from Matlab for 0.075';

xlswrite(Excel_title,column_headers,'Contact Area (mm^2)','A1');
xlswrite(Excel_title,row_headers,'Contact Area (mm^2)','A2');
xlswrite(Excel_title,CA_mean_Intact,'Contact Area (mm^2)','B2');
xlswrite(Excel_title,CA_mean_Cut,'Contact Area (mm^2)','C2');

xlswrite(Excel_title,column_headers,'Average Pressure (MPa)','A1');
xlswrite(Excel_title,row_headers,'Average Pressure (MPa)','A2');
xlswrite(Excel_title,AP_mean_Intact,'Average Pressure (MPa)','B2');
xlswrite(Excel_title,AP_mean_Cut,'Average Pressure (MPa)','C2');

xlswrite(Excel_title,column_headers,'Peak Pressure (MPa)','A1');
xlswrite(Excel_title,row_headers,'Peak Pressure (MPa)','A2');
xlswrite(Excel_title,PP_mean_Intact,'Peak Pressure (MPa)','B2');
xlswrite(Excel_title,PP_mean_Cut,'Peak Pressure (MPa)','C2');

xlswrite(Excel_title,column_headers,'Average Force (N)','A1');
xlswrite(Excel_title,row_headers,'Average Force (N)','A2');
xlswrite(Excel_title,AF_mean_Intact,'Average Force (N)','B2');
xlswrite(Excel_title,AF_mean_Cut,'Average Force (N)','C2');
```

```
%% File Notes and Purpose
%Author: Nolan Norton
%University of Kansas Bioengineering
%Created: March/April 2018
%Version number: 1
%Purpose: Calculate the Contact Area, Average Pressure, Average Force, and
%Peak Pressure from the input pressure data.
%Input Data Format: The imported data should be in an excel file in cells
A1:F6 and
%each frame should be written in a seperate tab.

%% Function

function [Area, Avg_P, Avg_F, Peak_P] = parameter_calculation(data)

%Threshold indexing if a manual threshold is used
global threshold;
idx = find(data >= threshold);

%Threshold indexing if a defined standard deviation method is used
% data_column = data(:); %Puts all of the values in the variable data into a
column vector
% frame_mean = mean(data_column); %Finds the mean value of the pressure for a
frame
% SD = std(data_column,1); %Finds the standard deviation of the pressure
values in the frame
% difference = abs(frame_mean-SD);
% idx = find(data >= difference); %This finds the indices of the all of the
values that are equal to or above the specified threshold (in this case the
threshold is 0.3)

%Thresholding and calculating the parameters
thres_data = data(idx); %Plugs the indices into the original matrix and puts
them in order (by index) into a column array to give a thresholded pressure
array.
Area = length(thres_data)*3.623;  %3.623 is the area in square millimeters
per sensel
Avg_P = mean(thres_data);  %Finds the average pressure, or the (total force
over contact area)/(contact area). This method is identical to finding the
total force sum and then dividing by Area.
Avg_F = Avg_P*Area;  %Finds the average pressure of the thresholded data.
Peak_P = max(thres_data);  %Finds the value of the largest element of the
thresholded pressure data.

%Extra verification that the above methods are equivalent to the
%way that Tekscan calculates values
F = thres_data*3.623;  %Multiplies each element in the thresholded pressure
array by the area of one sensel to give an array of the thresholded force
values
Total_F = sum(F);  %Gives a sum of the array to state the total force
Avg_P_Check = Total_F/Area;  %A check for the mean method. This is the way
that Tekscan defines Contact Pressure.
check_P = abs(Avg_P_Check-Avg_P);
if check_P >= 0.1
    disp('Significant difference between Avg_P methods');
end
```

```
%Check for the Avg_F calculation
check_F = abs(Avg_F-Total_F);
if check_F >= 0.1
    disp('Significant difference between Avg_F methods');
end

end
```